Journal of Paleontology, 97(2), 2023, p. 477–498

0022-3360/23/1937-2337
doi: 10.1017/jpa.2022.103

JOURNAL OF PALEONTOLOGY
A PUBLICATION OF THE Paleontological SOCIETY

New paromomyids (Mammalia, Primates) from the Paleocene of southwestern Alberta, Canada, and an analysis of paromomyid interrelationships

Craig S. Scott,[1] Sergi López-Torres,[2,3] Mary T. Silcox,[4]* and Richard C. Fox[5,†]

[1]Royal Tyrrell Museum of Palaeontology, P. O. Box 7500, Drumheller, Alberta T0J 0Y0, Canada <craig.scott@gov.ab.ca>
[2]University of Warsaw, Faculty of Biology, Biological and Chemical Research Centre, Institute of Evolutionary Biology, Żwirki i Wigury 101, Warsaw 02-089, Poland <s.lopez-torres@uw.edu.pl>
[3]Division of Paleontology, American Museum of Natural History, 200 Central Park West, New York, New York 10024, USA <slopez-torres@amnh.org>
[4]Department of Anthropology, University of Toronto Scarborough, 1265 Military Trail, Scarborough, Ontario M1C 1A4, Canada <mary.silcox@utoronto.ca>
[5]Laboratory for Vertebrate Paleontology, Department of Biological Sciences, University of Alberta, Edmonton, Alberta T6G 2E9, Canada <richard.fox@ualberta.ab.ca>

Abstract.—Paromomyidae are one of several families of plesiadapiforms that flourished during the Paleocene in North America soon after the extinction of non-avian dinosaurs some 66 million years ago. Although they are often among the best-represented plesiadapiforms in mammalian faunas in both North America and Europe, the early history of paromomyids is poorly understood, and their fossil record at higher latitudes is comparatively depauperate. We report here on the discovery of two new species of paromomyids from Paleocene deposits in southwestern Alberta: *Edworthia greggi* new species is the second known species of the basal paromomyid *Edworthia* Fox, Scott, and Rankin, 2010 whereas *Ignacius glenbowensis* new species is among the most abundantly represented species of *Ignacius* Matthew and Granger, 1921. These new discoveries document, for the first time, parts of the upper dentition of *Edworthia*, and the new species of *Ignacius* represents the first new, pre-Clarkforkian species of the genus to be described in nearly 100 years. A comprehensive phylogenetic analysis of nearly all known paromomyid taxa (including the new species described herein) recovered both species of *Edworthia* near the base of the paromomyid tree in a polytomy with *Paromomys depressidens* Gidley, 1923 and a paraphyletic *Ignacius*. The new paromomyids from Alberta not only increase the known taxonomic diversity of *Edworthia* and *Ignacius* but also add significantly to knowledge of the dental anatomy of these poorly known genera and further add to a uniquely Canadian complement of Paleocene plesiadapiforms.

UUID: http://zoobank.org/a2f31cfe-09b9-4168-b09f-9d0c3d0af342

Introduction

Paromomyidae Simpson, 1940 constitutes one of several families of early primates collectively referred to as plesiadapiforms, a group of Paleocene- to Eocene-age mammals that have been regarded either as a sister clade to Euprimates Hoffstetter, 1977 as a non-monophyletic assemblage of stem primates or as primitive euarchontans (see, e.g., Beard, 1993; Bloch et al., 2007; Silcox and Gunnell, 2008; Boyer et al., 2010; Fox, 2011; Silcox and Williamson, 2012; Ni et al., 2013; Chester et al., 2015; Silcox et al., 2020). Paromomyidae are one of several plesiadapiform families that appear soon after the extinction of non-avian dinosaurs, first known in the Torrejonian North American Land Mammal Age (NALMA) where, along with the Picrodontidae, Palaechthonidae, Carpolestidae, and Plesiadapidae, they began what has been considered the first major adaptive radiation of Primates (Silcox and Gunnell, 2008; Clemens and Wilson, 2009; Silcox and Williamson, 2012; Silcox et al., 2017). As currently construed, the Paromomyidae include six named North American genera (*Paromomys* Gidley, 1923; *Edworthia* Fox, Scott, and Rankin, 2010; *Ignacius* Matthew and Granger, 1921; *Phenacolemur* Matthew, 1915; *Elwynella* Rose and Bown, 1982; *Acidomomys* Bloch et al., 2002), the European genus *Arcius* Godinot, 1984, and as yet unnamed genera from the Eocene Wutu Formation of China (Tong and Wang, 1998, 2006) and the Eureka Sound Formation of Ellesmere Island in the Canadian Arctic (West and Dawson, 1977; Eberle and Greenwood, 2012; Miller and Beard, 2020). Although there is considerable diversity among the various paromomyid genera, the family can be characterized generally as having upper molars with small conules and a relatively well-developed postprotocone fold and talon basin, a tall and

[†]Deceased
*Corresponding author

premolariform p4, and low-crowned lower molars with a strongly anteriorly leaning trigonid, a weak paraconid, and a shallow protocristid notch (Bown and Rose, 1976; Silcox and Gunnell, 2008; Silcox et al., 2008; Fox et al., 2010). The few well-preserved paromomyid crania suggest that the snout is long, the orbits are laterally positioned, a postorbital bar is lacking, the inflated auditory bulla is composed of the entotympanic alone, and parts of the internal carotid artery and nerve were housed in a groove or bony tube at the lateral extremity of the promontorium (Kay et al., 1992; Bloch and Silcox, 2001; Silcox, 2003; Silcox and Gunnell, 2008; López-Torres et al., 2018). Postcranially, paromomyids have adaptations that are suggestive of arborealism (Boyer and Bloch, 2008). Although paromomyids have been variously allied with different plesiadapiforms, particularly the plesiadapoids (see, e.g., Gingerich, 1976; Gunnell, 1989), contemporary analyses suggest the family may have shared a recent common ancestry with picrodontids and several palaechthonids, resulting in their current classification in the Paromomyoidea (Simpson, 1940) (see Silcox et al., 2008; Chester et al., 2017).

Paromomyids are important in several regards. The family is the longest-lived group of plesiadapiforms, ranging in age from the early Paleocene (Torrejonian) to the late Eocene (Chadronian), and constitutes the only plesiadapiforms represented from both Europe and Asia, in addition to North America (Godinot, 1984; Tong and Wang, 1998; Aumont, 2004; Silcox and Gunnell, 2008; Silcox et al., 2008, 2017; Kihm and Tornow, 2014; note that we do not consider purported plesiadapids from Pakistan and China to be referable to Plesiadapidae—see discussion in Silcox, 2008). In North America, paromomyids are geographically widespread, with specimens from as far south as the Big Bend area of southern Texas and north to the Canadian Arctic (Schiebout, 1974; Dawson et al., 1976; West and Dawson, 1977; McKenna, 1980; Silcox and Gunnell, 2008; Eberle and Greenwood, 2012; Silcox and Williamson, 2012; Miller and Beard, 2020). This North American geographic range has figured importantly in recent analyses of early primate distributional patterns, the results of which suggest that at least some plesiadapiforms were continentally more widespread during the early Paleocene than previously thought, contrasting with many other archaic eutherians that show higher levels of endemism (Silcox and Williamson, 2012). In addition to their widespread North American occurrence, the record of paromomyids can in many instances be locally dense, allowing detailed studies of species-level variation and small-scale, within-basin evolution (e.g., Silcox et al., 2008). Last, several paromomyid genera are known from exceptionally well-preserved specimens, permitting unprecedented insight into cranial anatomy and evolution and the evaluation of competing hypotheses regarding the functional morphology of the postcranial skeleton (e.g., Rose and Gingerich, 1976; Kay and Cartmill, 1977; Kay et al., 1992; Bloch and Silcox, 2001; Bloch et al., 2002; Boyer and Bloch, 2008; Silcox et al., 2009, 2017).

Despite the relatively dense paromomyid record, the early history of the family remains poorly understood. For example, although the most plesiomorphic genus, *Paromomys*, is known from four species (*Pa. depressidens* Gidley, 1923; *Pa. maturus* Gidley, 1923; *Pa. farrandi* Clemens and Wilson, 2009; *Pa. libedianus* Silcox and Williamson, 2012) that range from the early Torrejonian through the earliest part of the Tiffanian (Silcox and Gunnell, 2008; Clemens and Wilson, 2009), they are known exclusively from isolated teeth and incomplete jaws with teeth; two of these (*Pa. farrandi* and *Pa. libedianus*) are represented by very limited material, and in none is the complete dentition known. Likewise, the earliest species of *Ignacius*, *I. fremontensis* (Gazin, 1971), is known with certainty only from the type locality in south-central Wyoming (Gunnell, 1989), whereas other supposed occurrences of the species are represented by very small samples, prompting only tentative identifications (e.g., Rose, 1981; Fox, 1990). Further, the early occurrence of the most recently discovered paromomyid genus, *Edworthia* (itself known from limited material), suggests that paromomyid diversity during the early part of the radiation of the family was even greater than previously documented (Fox et al., 2010). Taken together, these facts suggest that although the Paromomyidae are of great importance in understanding the initial radiation of plesiadapiforms in North America during the Paleocene, their early history is obscure.

We describe herein new species of two early paromomyids from several localities in the Porcupine Hills and Paskapoo formations of Alberta, ranging from the ?middle Torrejonian (To2) to the earliest Tiffanian (Ti1) (Fig. 1; Youzwyshyn, 1988; Fox, 1990, 2011; Scott et al., 2002, 2013; Scott, 2003). These new discoveries document, for the first time, parts of the upper dentition of *Edworthia*, the features of which further distinguish this genus from other paromomyids and confirm its relatively basal position in the family, and a new species of *Ignacius* that represents the first new, pre-Clarkforkian species of the genus to be described in nearly 100 years. The new paromomyids from Alberta not only increase the known taxonomic diversity of *Edworthia* and *Ignacius* but also add significantly to knowledge of the dental anatomy of these poorly known genera and further add to a uniquely Canadian complement of Paleocene plesiadapiforms (Fox, 2011).

Geological setting

Regional geology.—The fossils described herein were discovered at localities in the Paskapoo Formation in the Calgary and Cochrane areas of southwestern Alberta (Fig. 1). The Paskapoo Formation is a large unit of Paleocene-age continental rock occurring in the plains and foothills of southwestern and west-central Alberta (Jerzykiewicz, 1997; Hamblin, 2004). The formation is primarily fluvial in origin and is dominated by buff-weathering sandstone, with subordinate gray to greenish siltstone and mudstone, and commercially significant deposits of coal (Hamblin, 2004). The Paskapoo Formation is highly fossiliferous and documents mammalian faunas that range in age from the early Paleocene (To2 or older) to the later parts of the late Paleocene (Ti5) (e.g., Russell, 1926, 1929, 1967; Rutherford, 1927; Youzwyshyn, 1988; Fox, 1990; Scott et al., 2002; Scott, 2003, 2008, 2010).

Locality information.—Who Nose?, the oldest locality included in this study, is exposed at a cutbank on West Nose Creek in the north part of the city of Calgary (Scott, 2003). Fossil mammals documented at the locality, including the plesiadapid *Pronothodectes matthewi* Gidley, 1923, suggest that the local

https://doi.org/10.1017/jpa.2022.103 Published online by Cambridge University Press

Figure 1. Generalized map of southern Alberta, Canada. Numbers indicate the localities where specimens of *Edworthia greggi* n. sp. and *Ignacius glenbowensis* n. sp. have been discovered. 1 = Who Nose? locality (early Paleocene, To2); 2 = Trainspotting locality (late Paleocene, Ti1); 3 = Cochrane 2 locality (late Paleocene, Ti1); 4 = Cochrane 1 locality (late Paleocene, Ti1). All localities occur in the Paskapoo Formation. Gray area represents approximate corporate boundaries of Calgary and Cochrane. Maps modified from http://d-maps.com/carte.php?num_car=67373&lang=en.

fauna is middle Torrejonian (To2) in age (*Protoselene opisthacus*/*Mixodectes pungens* Interval Zone of Lofgren et al., 2004), although conflicting results from magnetostratigraphic and palynological analyses suggest that the locality may be older, possibly in sediments correlated with magnetochron 28r (Lerbekmo and Sweet, 2000). Three localities from the Cochrane area west of Calgary are all of earliest Tiffanian age (*Plesiadapis praecursor*/*Pl. anceps* Lineage Zone; Lofgren et al., 2004), with the index taxon *Ectocion collinus* Russell, 1929 known from each. The Trainspotting locality (TMP locality L2402) occurs on the north side of Bow River east of Cochrane in Glenbow Ranch Provincial Park; the locality occurs near the base of magnetochron 26r and is accordingly very early in Ti1 (Lerbekmo and Sweet, 2000; Scott, 2019). Cochrane 1 (TMP locality L2382) occurs on the north side of Bow River in the town of Cochrane (two productive horizons have been discovered at Cochrane 1, with the fossils described in this study having come from the lower level). The Cochrane 2 locality occurs at a rail cut at the eastern edge of the town of Cochrane and documents one of the most diverse mammalian assemblages of the early part of the late Paleocene (Youzwyshyn, 1988; Fox, 1990; Scott et al., 2002); the locality is approximately 100 m higher stratigraphically than Cochrane 1 (Russell, 1929; and see Scott et al., 2013). Locality coordinates are on file at the Royal Tyrrell Museum of Palaeontology and available to qualified investigators.

North American Land Mammal Ages.—"Torrejonian," "Tiffanian," and "Clarkforkian" refer to several of the NALMAs of the Paleogene; NALMAs are biochrons, units of relative time defined by mammalian taxa that lived during those intervals (Woodburne, 2004).

Materials and methods

Dental terminology and measurements.—Dental nomenclature mostly follows Van Valen (1966) as modified by Szalay (1969); upper incisor nomenclature follows Gingerich (1976). Dental measurements were taken using Miyutomo digital calipers; orientation of teeth for measurement follows Clemens (1966).

Abbreviations for dentition.—C/c = upper/lower canine; I/I = upper/lower incisor; L = anteroposterior length; M/m = upper/lower molar; P/p = upper/lower premolar; W = labiolingual width.

https://doi.org/10.1017/jpa.2022.103 Published online by Cambridge University Press

Phylogenetic analysis.—A cladistic analysis was conducted to determine the phylogenetic relationships of *Edworthia greggi* n. sp. and *Ignacius glenbowensis* n. sp., and among paromomyids more broadly. The analysis included 25 described species of paromomyids, in addition to the two newly described species in the present study. Although the recently described *Arcius moniquae* (Godinot et al., 2021) was not included in our analysis, its exclusion would likely have little to no effect on the positions of *E. greggi* and *I. glenbowensis* given the robust sampling of *Arcius* in our dataset (i.e., six out of seven species represented). Non-paromomyid plesiadapiforms were included as immediate outgroups, including palaechthonids (*Premnoides* Gunnell, 1989, *Plesiolestes* Jepsen, 1930, *Torrejonia* Gazin, 1968, and *Palaechthon* Gidley, 1923), one micromomyid (*Foxomomys* Chester and Bloch, 2013), one microsyopid (*Navajovius* Matthew and Granger, 1921), and one purgatoriid (*Purgatorius* Van Valen and Sloan, 1965). A primitive eutherian, *Ukhaatherium nessovi* Novacek et al., 1997, was included as an outgroup to all plesiadapiforms. Given the paucity of cranial and postcranial data for paromomyids, the analysis included only dental characters, many of which were used in a recent analysis of European paromomyids (López-Torres and Silcox, 2018), while others were adopted from diagnoses in Matthew (1915), Matthew and Granger (1921), Gidley (1923), Simpson (1955), Russell et al. (1967), Gazin (1971), Godinot (1984), Robinson and Ivy (1994), Estravís (2000), Bloch et al. (2002, 2007), Secord (2008), Silcox et al. (2008), and Fox et al. (2010). Several characters that have been used previously in positing higher-level relationships of plesiadapiforms were also included (Silcox, 2001). Thirty-seven taxa were scored for 101 characters (Supplementary Data 1, 2). A parsimony analysis was conducted using PAUP 4.0*a165 (Swofford, 2002) using the following steps: (1) set *Ukhaatherium nessovi* as the only outgroup (Data > Define Outgroup…); (2) set selected characters as ordered (Data>Set Character Types; turn the following characters into ordered: 1, 12, 18, 31, 67, 72, 73, 83, 86, 92, and 93); (3) accept ordered characters (click "Done"); (4) set the type of analysis (Analysis > Heuristic search); (5) set the maximum number of trees to be saved to 1,000 (General > SetMaxTrees > 1,000); (6) set the number of replicates (reps) at 1,000 holding 1,000 trees at each step); (7) run the analysis (click OK).

Repository and institutional abbreviations.—UALVP, University of Alberta Laboratory for Vertebrate Paleontology, Edmonton, Alberta; TMP, Royal Tyrrell Museum of Palaeontology, Drumheller, Alberta.

Systematic paleontology

Order Primates Linnaeus, 1758
Superfamily Paromomyoidea Simpson, 1940
Family Paromomyidae Simpson, 1940
Genus *Edworthia* Fox, Scott, and Rankin, 2010

Type species.—*Edworthia lerbekmoi* Fox, Scott, and Rankin, 2010.

Other species.—*Edworthia greggi* new species.

Revised diagnosis.—Differs from *Paromomys* in its significantly smaller size and in having an anterior cingulum (although weak) and a well-developed metacone on P4, a single-rooted p2, more lingually positioned paraconid on m1, absence of an ectocingulid on the molar talonids, and relatively narrower lower molars with coronal walls that are not swollen. Differs from *Arcius* in having an anteriorly expanded parastylar region and lacking a postprotocrista on P4 and in lacking an expanded parastylar region on M1. Differs from *Phenacolemur* and *Ignacius* in lack of expanded posterolingual basin on P4. Differs from *Ignacius*, *Acidomomys*, and *Arcius* in having a weakly developed parastyle on P4. Differs from *Ignacius* in lack of V-shaped centrocrista on M1–2. Differs from *Arcius* in having anterocone taller than mediocone on I1 and expanded anterolabial corner on M3. Differs from *Ignacius*, *Acidomomys*, and *Paromomys* in having conules more appressed to the paracone and metacone on M1–2. Differs from *Ignacius*, *Phenacolemur*, *Arcius*, and *Paromomys* in having a larger paracone than metacone on M1–2. Differs from *Ignacius*, *Phenacolemur*, *Arcius*, and *Acidomomys* in having both conules and a deep cleft between the protocone and talon on M1–2. Differs from *Ignacius*, *Phenacolemur*, *Acidomomys*, *Elwynella*, and *Arcius* in retaining p2. Differs from *Ignacius*, *Acidomomys*, *Elwynella*, *Arcius*, and most species of *Phenacolemur* in retaining an ectocingulid on the molar trigonids. Diastema between the enlarged lower incisor and the cheek teeth absent, in contrast to *Phenacolemur*, *Arcius*, *Acidomomys*, and later-occurring species of *Ignacius*.

Edworthia greggi new species
Figures 2, 3; Table 1

2003 *Ignacius* cf. *I. fremontensis* (Gazin) in Scott, p. 755, fig. 4.32–4.36.

Holotype.—UALVP 44136, incomplete right dentary with p4, m2, m3 trigonid, and alveoli for i1, p2–3, m1, and m3 talonid (Fig. 3.1–3.4). Who Nose? locality, Paskapoo Formation of Alberta, early Paleocene (?middle Torrejonian, To2), *Protoselene opisthacus/Mixodectes pungens* Interval Zone of Lofgren et al. (2004).

Diagnosis.—Differs from *E. lerbekmoi* in having a narrower p4 that lacks a paraconid and in having a wider talonid relative to trigonid; lower molars have wider and more anteroposteriorly compressed trigonid with smaller paraconid that is more closely appressed to metaconid. Differs further from *E. lerbekmoi* in having molar talonid longer and wider, particularly on m2, with more anteriorly positioned entoconid.

Occurrence.—Type locality only.

Description.—

I1.—Although I1 is known for several paromomyids from associated or articulated specimens, including well-preserved skulls of *Ignacius* and *Acidomomys* (e.g., Godinot, 1984; Rose et al., 1993; Bloch et al., 2002, 2007; López-Torres and Silcox, 2018), little is known of this tooth position for geologically older

https://doi.org/10.1017/jpa.2022.103 Published online by Cambridge University Press

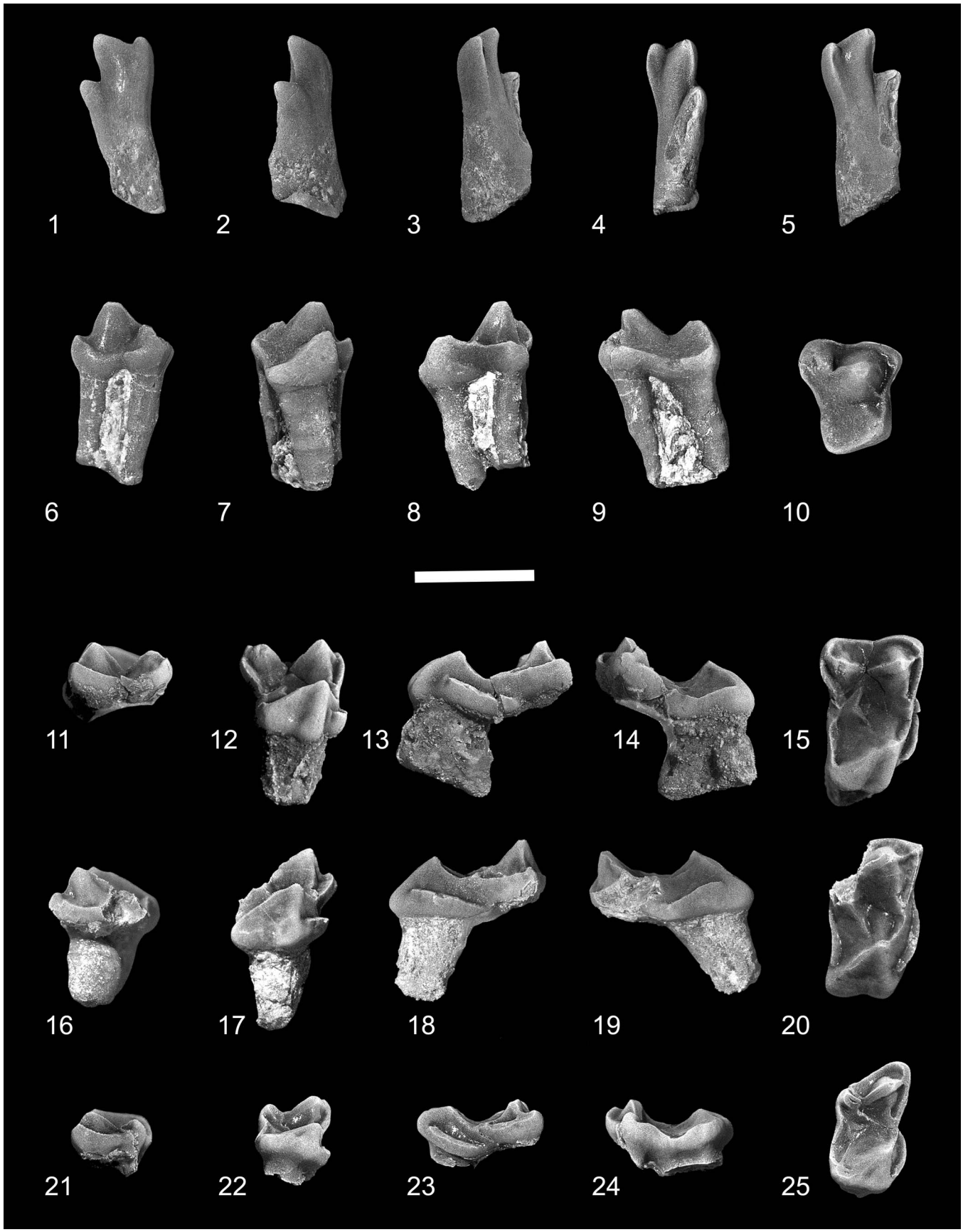

https://doi.org/10.1017/jpa.2022.103 Published online by Cambridge University Press

Figure 2. *Edworthia greggi* n. sp. from the Paskapoo Formation, early Paleocene, southwestern Alberta. (**1–5**) UALVP 44109, left I1: (**1**) dorsal view; (**2**) lateral view; (**3**) medial view; (**4**) occlusal view; (**5**) oblique occlusal view. (**6–10**) UALVP 43287, RP4: (**6**) labial view; (**7**) lingual view; (**8**) anterior view; (**9**) posterior view; (**10**) occlusal view. (**11–15**) UALVP 44076, LM1: (**11**) labial view; (**12**) lingual view; (**13**) anterior view; (**14**) posterior view; (**15**) occlusal view (all views reversed from original). (**16–20**) UALVP 43289, incomplete RM2: (**16**) labial view; (**17**) lingual view; (**18**) anterior view; (**19**) posterior view; (**20**) occlusal view. (**21–25**) UALVP 43293, RM3: (**21**) labial view; (**22**) lingual view; (**23**) anterior view; (**24**) posterior view; (**25**) occlusal view. Scale bar = 2 mm.

taxa such as *Paromomys* and *Edworthia*. UALVP 44109 was discovered in isolation; we refer this specimen to *Edworthia* on the basis of its similarity to I1 of other paromomyids, and to *Edworthia*, rather than *Paromomys* (also known from the Who Nose? locality; C.S.S., personal observation, 2022), on the basis of its comparatively small size. The crown of UALVP 44109 is elongate and slender, with the enamel extending farther posteriorly on the occlusal surface than on the anterodorsal surface. The crown supports three unequally developed apical cusps. The largest and tallest of these, the anterocone, is slightly curved, with the tip bending somewhat centrally and laterally. A mediocone arises from the anteromedial shoulder of the anterocone and is connected to the latter by a short, weak crest. The mediocone is about half the size and height of the anterocone and is slightly swollen, and its tip projects anteriorly and somewhat ventrally. A sharp crest, the mediocrista, arises from the medial side of the mediocone and progresses posterodorsally for about one-third of the crown before fading away; the mediocrista does not terminate in a prominent shelf as it does in other paromomyids (e.g., *Phenacolemur pagei* Jepsen, 1930; see Secord, 2008). An interdental facet is not developed on the medial side of the mediocone, suggesting that the opposing I1s did not meet. A third cusp, the laterocone, is developed posterolateral to the anterocone, about halfway between the base of the crown and the tip of the anterocone. The cusp is about two-thirds the size and height of the anterocone, and its apex projects in a manner similar to that of the anterocone. A sharp crest extends posterodorsally from the tip of the anterocone, terminating at the base of the laterocone. The crown narrows toward the base, and although worn and slightly chipped, a prominent ridge can be discerned, running from the laterocone along the lateral margin. A shallow, subcircular wear facet occurs posterior and medial to the laterocone, in a position where a posterocone is present in other paromomyids (see, e.g., Rose et al., 1993). Whether this was also the case in UALVP 44109 cannot be determined unequivocally, but what remains of the base of the crown and the relatively mild state of wear suggests that if a posterocone was originally present, it was likely very small and easily removed even after light wear.

P4.—The crown of P4 (UALVP 43287) is subtrapezoidal in occlusal outline, with long posterior and labial and shorter anterior and lingual sides. The stylar shelf is undeveloped, with the base of the paracone situated at the labial edge of the crown. A low but prominent ectocingulum extends posteriorly from the parastylar lobe, eventually turning ventrally toward the apex of the metacone before fading away. The paracone is large and conical, and a weak preparacrista extends from it a short distance anteriorly before terminating near the base of the cusp. A small, poorly developed parastyle is present at the junction of the ectocingulum and paracingulum. The metacone is smaller and lower than the paracone and is positioned somewhat labial to the level of the latter; as a result, the metastylar lobe bulges posteriorly and labially. The centrocrista is deeply notched, with the postparacrista oriented anteroposteriorly and the premetacrista running anterolingually–posterolabially; there is no postmetacrista. The protocone is lower than the paracone, but of about the same size at its base, and is situated close to the paracone. A sharp preprotocrista extends from the apex of the protocone toward the base of the paracone, where it meets the paracingulum and a short, posterolabially directed postparaconule crista, although the paraconule itself is undeveloped. The paracingulum continues labially to the anterolabial corner of the crown, where it joins the ectocingulum. A heavy postprotocone fold + posterior cingulum extends a short distance posterolingually from the apex of the protocone before curving labially toward the metastylar corner of the crown and forming a shallow, posteriorly sloping talon basin; a hypocone is not developed. A weak anterior cingulum is present.

M1.—The crown of M1 (UALVP 44076; Fig. 2.11–2.15) is subrectangular in occlusal outline, being much more transverse than long. The paracone is slightly larger and taller than the metacone, and they are joined by a widely notched centrocrista. The stylar shelf is scarcely developed, with only the low but prominent and shallowly invaginated ectocingulum present labially; as in P4, the ectocingulum on M1 extends posteriorly to the metacone before turning lingually to join the postmetacrista. A sharp preparacrista runs anteriorly from the paracone apex to join with the paracingulum + ectocingulum, but a parastylar cusp is not developed at their union. A distinct paraconule is not present, but a slight inflection of the enamel at the junction of the postparaconule crista and paracingulum may indicate its incipient presence. The metaconule is also represented by an inflection of enamel at the junction of the premetaconule crista and metacingulum, but here the inflection is substantially stronger than that of the paraconule. The protocone is anterior in position, with its anteriorly leaning apex nearly in line with that of the paracone; the cusp is slightly lower than the paracone and is significantly more anteroposteriorly compressed. A robust preprotocrista runs labially toward the paracone before joining the postparaconular crista + paracingulum; the postprotocrista is essentially indiscernible near the protoconal apex but becomes stronger as it nears the metaconule. The postprotocone fold + posterior cingulum sweeps posteriorly and lingually before turning abruptly labially to enclose a shallow talon basin, and the somewhat swollen lingual sides of the protocone and talon are separated by a shallow groove, imparting a mildly bilobed appearance to that part of the crown. The anterior cingulum is strongly developed, forming a shelf-like structure that runs from just dorsal of the protocone apex to the level of the paraconule.

M2.—The M2 of *Edworthia greggi* n. sp. is represented by UALVP 43289, and although the crown is damaged (the metastylar corner of the crown, metacone, and associated crests are missing), it nonetheless closely resembles M1, with the two differing mainly in the orientation of the preparacrista and postparacrista (a contrast typical in paromomyids between M1 and

https://doi.org/10.1017/jpa.2022.103 Published online by Cambridge University Press

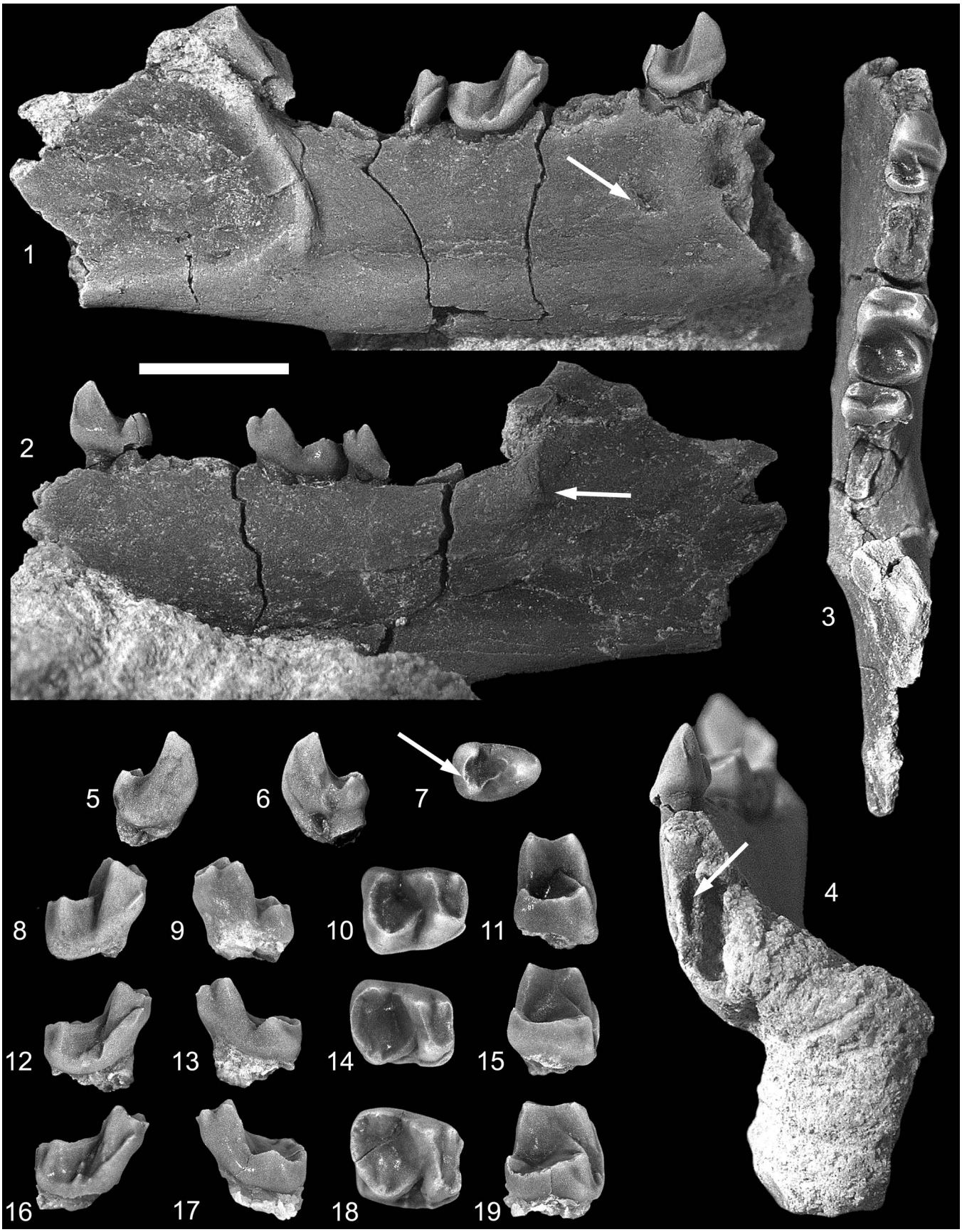

https://doi.org/10.1017/jpa.2022.103 Published online by Cambridge University Press

Figure 3. *Edworthia greggi* n. sp. from the Paskapoo Formation, early Paleocene, southwestern Alberta. (**1–4**) UALVP 44136, holotype, incomplete right dentary with p4, m2, and incomplete m3: (**1**) labial view (arrow points to posterior mental foramen); (**2**) lingual view (arrow points to tubercle at anteroventral limit of temporalis fossa); (**3**) occlusal view; (**4**) anterior view (arrow points to p2 alveolus). (**5–7**) UALVP 43288, Rp4: (**5**) labial view; (**6**) lingual view; (**7**) occlusal view (arrow points to hypoconulid). (**8–11**) UALVP 43291, Lm1: (**8**) labial view; (**9**) lingual view; (**10**) occlusal view; (**11**) posterior view (all views reversed from original). (**12–15**) UALVP 43290, Rm2: (**12**) labial view; (**13**) lingual view; (**14**) occlusal view; (**15**) posterior view. (**16–19**) UALVP 43304, Rm2: (**16**) labial view; (**17**) lingual view; (**18**) occlusal view; (**19**) posterior view. (**1, 2**) Some of the adhering matrix on UALVP 44136 was cropped for economy and ease of viewing. Scale bar = 2 mm.

M2; e.g., see Fig. 4.16). As in several other paromomyids (see, e.g., *Paromomys* and *Ignacius*; Szalay and Delson, 1979, figs. 18A, 19A), the preparacrista and postparacrista on M2 are oriented somewhat anterolabially, slightly oblique to the anteroposterior axis of the crown. In *Paromomys* and *Ignacius*, the paracone is somewhat labial to the level of the metacone on M2, but confirmation of this for *E. greggi* must await discovery of better-preserved M2s. The paraconule on M2, although still just an inflection of the enamel at the union of the postparaconular crista and paracingulum, is nonetheless better developed than on M1, and the postprotocrista is stronger, extending closer to the protocone apex.

M3.—The crown of M3 (UALVP 43293) is roughly rectangular in occlusal outline, being wider than long and having a weak constriction lingual to the paracone and metacone. The paracone is larger and taller than the metacone, and the two cusps are joined by a widely notched centrocrista; as in M2, the postparacrista is oriented anterolabially–posterolingually, oblique to the long axis of the crown. The stylar shelf is weakly developed labial to the paracone. A short preparacrista runs anterolabially from the paracone to the low ectocingulum, which extends posteriorly and then continues toward the apex of the metacone. As in M1 and M2, the conules on M3 are merely inflections of enamel at the union of the postparaconular crista + paracingulum and premetaconular crista + metacingulum. The protocone is lower and more anteroposteriorly compressed than the paracone, and its anteriorly leaning apex is in line with that of the latter. The preprotocrista is prominent, whereas the postprotocrista is virtually undeveloped. A well-developed postprotocone fold + posterior cingulum extends posteriorly from the protocone apex and then turns abruptly labially before continuing toward the metacone; the crest defines a shallow talon basin that juts slightly posteriorly past the level of the metastylar corner of the crown. As on M1 and M2, a heavy anterior cingulum is present on M3.

Table 1. Measurements and descriptive statistics for the dentition of *Edworthia greggi* n. sp. from the Who Nose? locality, Paskapoo Formation, southwestern Alberta, Canada. P = parameter; N = number; OR = observed range; MN = mean; SD = standard deviation; CV = coefficient of variation; P/p = upper/lower premolar; M/m = upper/lower molar; L = anteroposterior length; W = maximum crown width. Individual specimen measurements in Supplemental Data 3.

Element	P	N	OR	MN	SD	CV
P4	L	1	1.62	—	—	—
	W	1	1.90	—	—	—
M1	L	1	1.60	—	—	—
	W	1	2.61	—	—	—
M2	L	—	—	—	—	—
	W	1	2.50	—	—	—
M3	L	1	1.24	—	—	—
	W	1	2.24	—	—	—
p4	L	3	1.30–1.42	1.37	0.064	0.047
	W	3	0.90–1.00	0.97	0.058	0.060
m1	L	2	1.50–1.60	1.55	0.070	0.046
	W	2	1.30–1.42	1.36	0.085	0.062
m2	L	3	1.60–1.63	1.62	0.020	0.010
	W	3	1.30–1.50	1.42	0.11	0.075

Dentary.—The dentary in UALVP 44136 (holotype) is damaged, preserving only the horizontal ramus from p4 posteriorly to the anterior parts of the masseteric fossa and coronoid process. In most of its anatomy, the dentary of *Edworthia greggi* n. sp. resembles that of *E. lerbekmoi*, differing only in the position and development of mental foramina. In *E. greggi*, a large, dorsolaterally directed mental foramen occurs below the posterior root of p3 in a position similar to that reported by Szalay (1973) for *Paromomys maturus*. A second, smaller, foramen is developed posteroventral to the mental foramen; its aperture is slit-like and faces dorsolaterally. The posterior parts of the dentary are better preserved in UALVP 44136 than in UALVP 50989 (holotype of *E. lerbekmoi*) and thus provide some additional information about this part of the jaw in *Edworthia*. Like that in *E. lerbekmoi*, the masseteric fossa in *E. greggi* is relatively deep and long, and its anterior extent is bounded by a heavy, raised masseteric crest. Medially, the poorly excavated temporalis fossa is separated from the pterygoideus fossa ventrally by a faint crest; a prominent tubercle is developed at the anteroventral limit of the temporalis fossa.

The anteriormost parts of the dentary in UALVP 44136 preserve a bilaterally compressed alveolus that is here interpreted to have housed an enlarged lower incisor, similar to that in *E. lerbekmoi* and other paromomyids more generally. The alveolus is incomplete anteriorly, and its full course in the dentary cannot be determined; nonetheless, its trajectory resembles that seen in the dentary of *E. lerbekmoi*, sloping posteroventrally at an angle of about 45° from horizontal (Fox et al., 2010) to a point beneath, or more likely posterior to, the level of p4 (owing to the fragile nature of the specimen, the dentary has not been removed from the surrounding rock, which obscures the posteriormost parts of the i1 alveolus). As in *E. lerbekmoi*, the size and disposition of this alveolus in *E. greggi* suggests that it housed the anteriormost tooth in the lower jaw, here interpreted to be i1; its trajectory, like that in *E. lerbekmoi*, indicates that the tooth was held in a more nearly vertical position, rather than subhorizontal as in most other paromomyids (Fox et al., 2010). Three alveoli intervene between the i1 alveolus and p4, with the posterior two having roots in place. These posterior alveoli held p3, a tooth that is present in *Paromomys* and a few other paromomyids, including *Edworthia* (see, e.g., Gazin, 1971; Bloch et al., 2002; Fox et al., 2010). The size and spacing of the p3 roots suggest that the tooth was slightly smaller than p4. The anterior of the three alveoli is much smaller than either of the p3 roots: the alveolus has been "squeezed" to the lateral side of the dentary by the enlarged i1 alveolus, occupying only about half the width of the dentary, and it is shallow, terminating at about half the depth of the dentary (Fig. 3.4, arrow). Given its position immediately anterior to the p3 alveoli,

https://doi.org/10.1017/jpa.2022.103 Published online by Cambridge University Press

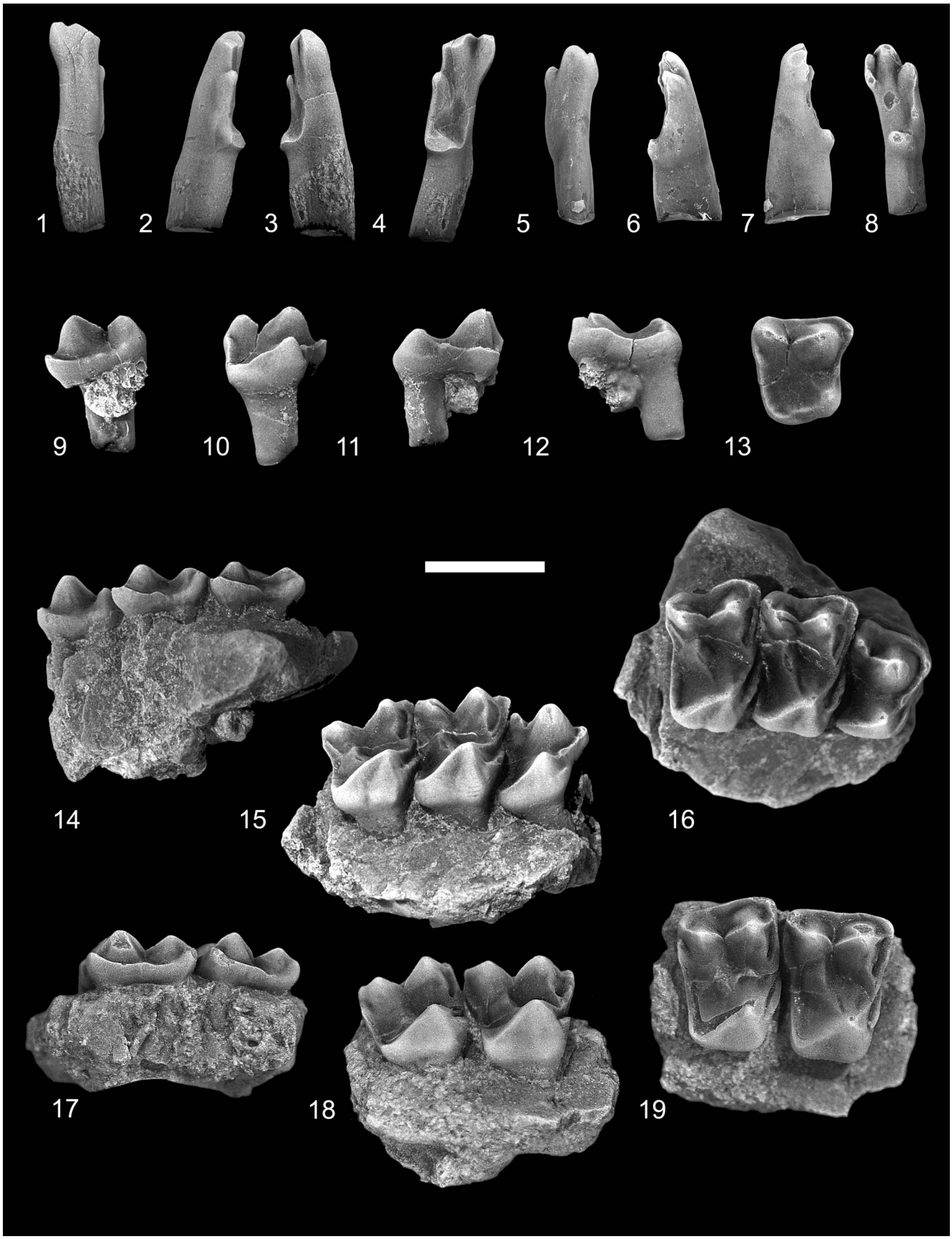

https://doi.org/10.1017/jpa.2022.103 Published online by Cambridge University Press

Figure 4. *Ignacius glenbowensis* n. sp. from the Paskapoo Formation, late Paleocene, southwestern Alberta. (**1–4**) TMP 2016.039.0056 (TS), RI1: (**1**) dorsal view; (**2**) lateral view; (**3**) medial view; (**4**) occlusal view. (**5–8**) TMP 2017.035.0052 (C1), LI1: (**5**) dorsal view; (**6**) lateral view; (**7**) medial view; (**8**) occlusal view. (**9–13**) TMP 2015.069.0136 (TS), RP4: (**9**) labial view; (**10**) lingual view; (**11**) anterior view; (**12**) posterior view; (**13**) occlusal view. (**14–16**) TMP 2017.025.0452 (TS), holotype, incomplete right maxilla with P4, M1–2: (**14**) labial view; (**15**) lingual view; (**16**) occlusal view. (**17–19**) UALVP 60942 (C2), incomplete left maxilla with M1–2 : (**17**) labial view; (**18**) lingual view; (**19**) occlusal view (all views reversed from original). TS = Trainspotting locality; C1 = Cochrane 1 locality; C2 = Cochrane 2 locality. Scale bar = 2 mm.

we interpret this alveolus to have housed a single-rooted p2, similar, albeit smaller, to its homologue in *E. lerbekmoi*.

p4.—The p4 is taller than m1 or m2 in UALVP 44136 but is slightly shorter and considerably narrower than that of *Edworthia lerbekmoi*. The crown is dominated by a tall and faintly recurved protoconid, having mildly inflated labial, lingual, and anterior sides and a flat and sheer postvallid wall. A weak paracristid descends anteriorly from the protoconid apex to a level approximately two-thirds the height of the protoconid, at which point it becomes stronger and turns slightly lingually as it nears the base of the cusp. The paracristid can either fade away as it approaches the base of the protoconid (e.g., UALVP 44153) or continue posteriorly as a faint lingual cingulid (e.g., UALVP 44136; Fig. 3.2). Neither paraconid nor metaconid is developed. The shallowly basined talonid is slightly wider than the protoconid at its base, but only about half its length, and it supports two well-developed, bulbous cusps. The hypoconid is low, whereas the entoconid is both larger and taller and positioned slightly posterior to the level of the hypoconid; a minute hypoconulid is present on one specimen (UALVP 43288; Fig. 3.7, arrow), situated very close to the hypoconid. The cristid obliqua is low and short and meets the postvallid wall at, or labial to, the anteroposterior midline; as a result, the hypoflexid can be shallow (e.g., UALVP 44153) or relatively deeper (e.g., UALVP 44136; Fig. 3.2, 3.3). As in p4 of *E. lerbekmoi*, the entocristid is undeveloped in *E. greggi* n. sp., and the talonid is open lingually. Moderate exodaenodonty is developed at the posterior root, and an ectocingulid is not present.

m1.—The crown of m1 (UALVP 44136, 43291) is subtrapezoidal in occlusal outline, with the talonid being wider than the trigonid. As in paromomyids generally, the trigonid is somewhat anteroposteriorly compressed and canted anteriorly and is subrectangular in occlusal outline. The paraconid is low and conical, close to but separate from the metaconid, and positioned just labial of the lingual margin of the crown. The paracristid descends steeply anteriorly from the protoconid apex before turning sharply lingually, forming a low shelf as it extends to the paraconid. The protoconid and metaconid are subequal in height, but the metaconid is the more massive cusp; the two are joined by a high, sharp, and shallowly notched protocristid. A moderately well-developed metastylid crest extends from the apex of the metaconid ventrally to the talonid notch. The talonid basin is about as wide as long, shallow, and lingually sloped, with its deepest point occurring just labial to the talonid notch. The hypoconid is low and positioned posterolabially, while the entoconid is directly opposite the hypoconid and slightly lower. A minute hypoconulid is developed posterolingual to the hypoconid and labial of the anteroposterior midline; as a result, the hypocristid is short, whereas the postcristid is considerably longer and forms the majority of the posterior rim of the talonid. The cristid obliqua meets the postvallid wall slightly labial of the anteroposterior midline and can continue toward the apex of the metaconid (e.g., UALVP 43303) or quickly fade away (e.g., UALVP 43291; Fig. 3.10), a situation owing, at least in part, to differential wear on the specimens. The entocristid is short and low, and the talonid notch is relatively shallow. As in *E. lerbekmoi*, a sharp but abbreviated ectocingulid is developed in *E. greggi* n. sp., extending posteriorly from beneath the protoconid arm of the paracristid to the hypoflexid whereupon it abruptly ends; a small cuspule can be present on the hypoflexid shelf.

m2.—The m2 resembles the m1 in most of its major features but differs in several important ways. The crown of m2 is larger than that of m1, the trigonid and talonid are both wider, and the trigonid is lower, both in absolute terms and relative to the height of the talonid. As is typical of paromomyid m2s compared with m1s, the trigonid is considerably more anteroposteriorly compressed than on m1, with the paracristid and protocristid longer and the paraconid higher, more lingual in position, and more closely appressed to the metaconid. In addition to being considerably longer and wider, the talonid on m2 is shallower than on m1, the hypoconid is lower, and the hypoconulid is scarcely developed. As in m1, the entoconid on m2 is directly opposite the hypoconid. The cristid obliqua contacts the postvallid wall more labially and at a point more dorsal than on m1, although the crest does not continue on toward the apex of the metaconid. The ectocingulid on m2 is better developed than on m1, and it continues on to the talonid (Fig. 3.12, 3.16).

m3.—Little can be said about the m3 as it is known only by its trigonid. Compared with m1 and m2, the m3 trigonid is even more anteroposteriorly compressed, the paraconid is more lingual in position and more closely appressed to the metaconid, and the cristid obliqua contacts the postvallid wall more labially. Further, the remnant of the posterior root indicates that the talonid is considerably longer than the trigonid and longer than that in the more anterior molars.

Etymology.—Named in honor of the late Dr. Gregg F. Gunnell.

Materials.—UALVP 44109, I1; UALVP 43287, P4; UALVP 44076, M1; UALVP 43289, M2; UALVP 44237, incomplete M1 or M2; UALVP 43293, M3; UALVP 44236, incomplete M3; UALVP 44153, 43288, p4; UALVP 43291, 43303, 44138, m1; UALVP 43290, 43292, 43304, 44139, m2; UALVP 44198, 44230, incomplete m3.

Remarks.—In his study of the mammals from the Who Nose? locality, Scott (2003) referred several teeth tentatively to *Ignacius fremontensis*, noting that while the similarities with this species were generally strong, several unusual features precluded a definitive referral. Many of these differences (e.g., prominent anterior cingulid on lower molars, more lingual molar paraconid, weaker hypoconal shelf) were interpreted as

https://doi.org/10.1017/jpa.2022.103 Published online by Cambridge University Press

plesiomorphic (being shared with species of *Paromomys*), and it was implied that with further sampling these may prove taxonomically important. Subsequent collections from Who Nose? resulted in the discovery of additional specimens that were referable to the same species, and with the publication of the first specimens of *Edworthia* from the nearly co-eval Edworthy Park locality (Fox et al., 2010), the distinctiveness of the Who Nose? paromomyid became clear.

Comparison with *Edworthia lerbekmoi*.—Although *E. greggi* n. sp. closely resembles *E. lerbekmoi* in most features of the dentition (including the orientation of the i1 alveolus, which indicates that the i1 was held in an oblique, rather than subhorizontal, position), several consistent differences indicate the two are not conspecific. For example, the trajectory of the p2 alveolus is more anteriorly leaning than in *E. lerbekmoi*, suggesting that the tooth was somewhat more procumbent, and the p2 is likely smaller, as inferred from the dimensions of the alveolus. The paraconid and ectocingulid are undeveloped on p4 of *E. greggi*, and the protoconid is slightly more anteriorly leaning; the entoconid is taller and more anteriorly positioned, and there is greater exodaenodonty at the posterior root. The strongest differences, however, occur on the lower molars, particularly on m2, where the trigonid is more anteroposteriorly compressed, and the paraconid is smaller and more closely appressed to the metaconid apex. The talonid is longer relative to width on both m1 and m2 of *E. greggi*, with the rim being more nearly circular in outline (rather than rectangular), the entoconid is more anterior, and the hypoconulid is very weak or undeveloped.

Genus *Ignacius* Matthew and Granger, 1921

Type species.—*I. frugivorus* Matthew and Granger, 1921.

Other species.—*I. fremontensis* (Gazin, 1971); *I. graybullianus* Bown and Rose, 1976; *I. clarkforkensis* Bloch et al., 2002.

Ignacius glenbowensis new species
Figures 4–7; Table 2

Holotype.—TMP 2017.025.0452, incomplete right maxilla with P4, M1–2 (Fig. 4.14–4.16). Trainspotting locality, Paskapoo Formation of Alberta, late Paleocene (earliest Tiffanian, Ti1), *Plesiadapis praecursor*/*Plesiadapis anceps* Lineage Zone of Lofgren et al. (2004).

Diagnosis.—Differs from *I. fremontensis* in M1 and M2 having weaker paraconule, more lingually and posteriorly extended talon, and in lingual wall being more inflated and less bilobate; m2 paraconid smaller and more lingual, and talonid anteroposteriorly shorter and wider relative to trigonid; m3 hypoconulid lobe better developed. Differs from *I. frugivorus* in P4 having weaker metacone and talon, resulting in rectangular rather than square occlusal outline; molar stylar shelf wider, paracone and metacone more closely approximated, talon weaker, occlusal outline more rectangular (rather than square); p4 absolutely smaller; molar talonid shorter and narrower, m3 hypoconulid lobe generally less well developed. Differs from *I. graybullianus* in P4 having generally better-developed parastylar lobe and in talon being less posterolingually expanded; M2 larger relative to M1, molar talon less posterolingually expansive; p4 larger relative to m1, molar paraconid stronger. Differs from *I. clarkforkensis* in P4 with considerably weaker talon, generally better-developed parastylar lobe; M2 larger relative to M1, molars with wider stylar shelf, M3 with considerably less posteriorly expanded talon; m1 and m2 with stronger paraconid, relatively deeper and less angular talonid basin, entoconid relatively smaller and more lingually projecting.

Occurrence.—Late Paleocene (earliest Tiffanian, Ti1), *Plesiadapis praecursor*/*Plesiadapis anceps* Lineage Zone of Lofgren et al. (2004).

Description.—

I1.—The incisors referred here to *Ignacius glenbowensis* n. sp. were discovered in isolation; they are referred to this species on the basis of their overall similarity with I1s of other paromomyids, size, and an absence of compelling evidence for the presence of an additional paromomyid in any of the included mammalian faunas where *I. glenbowensis* occurs. As in those of other paromomyids, the crown of I1 in *Ignacius glenbowensis* is elongate and slender, with the enamel extending farther posteriorly on the occlusal and lateral surfaces than on the anterodorsal and medial surfaces. The anterocone is large and somewhat dorsoventrally compressed, and the tip projects centrally and laterally. The mediocone, arising from a relatively anterior position on the anterocone, varies in its size: in one specimen (TMP 2016.039.0056; Fig. 4.4), it is about half the size and height of the anterocone, whereas in another (TMP 2017.035.0052; Fig. 4.8), it is slightly smaller than one-third the size; in both specimens, the cusp is connected to the anterocone by a sharp, V-shaped crest. The mediocone is swollen, especially so in TMP 2016.039.0056, with the exception of the medial side, which is flattened; a prominent interdental facet is developed here, indicating the opposing I1s met at the midline. The apex of the mediocone projects anteriorly and ventrally. The mediocrista arises from the medial side of the mediocone and progresses a short distance posterodorsally before weakening and eventually fading away. The laterocone arises a short distance posterolateral to the anterocone and, like the mediocone, varies in its development: in one specimen (TMP 2017.035.0052; Fig. 4.4) it is subequal in size and height to the anterocone, whereas in another (TMP 2016.039.0056; Fig. 4.8) it is significantly smaller; its apex projects anteriorly and ventrally. A sharp crest extends anterodorsally from the tip of the laterocone, meeting a similar crest running posterodorsally from the anterocone. A prominent, dorsally convex crest extends posteriorly from the laterocone along the lateral margin of the crown before turning medially and terminating at a low, undivided posterocone. Wear is present on the apices of each of the major cusps, with the anterocone having been worn down to nearly half of its original height and the posterocone having been nearly removed in one specimen (TMP 2016.039.0056, Fig. 4.4). A slightly concave wear facet occurs centrally on the occlusal surface, near the bases of the anterocone and laterocone, presumably from occlusion with the i1.

P4.—The P4 of *Ignacius glenbowensis* n. sp. is known from several specimens, including the holotype. The tooth is

https://doi.org/10.1017/jpa.2022.103 Published online by Cambridge University Press

three-rooted and the crown subtrapezoidal in occlusal outline, with long labial, shorter lingual, and subparallel anterior and posterior sides. A swollen, conical paracone dominates the labial side of the crown, occupying nearly half the length and width of the crown; a smaller and lower metacone occurs posterior and slightly labial to the paracone, with the two cusps connected by a low, sharply notched, asymmetrical centrocrista, with the postparacrista longer than the premetacrista. The stylar shelf is undeveloped, with the labial margin of the crown consisting of only a heavy ectocingulum. The faint preparacrista extends anteriorly where it meets the ectocingulum and paracingulum. The parastylar lobe is variably developed: in some specimens (e.g., TMP 2017.025.0452; Fig. 4.16), the lobe is smoothly rounded, whereas in others (e.g., TMP 2015.069.0136; Fig. 4.13), it is drawn out anteriorly as a distinct spur; in either case, a parastyle is not present. The metacone is somewhat offset labially from the level of the paracone, and the premetacrista is oriented anterolingually–posterolabially; consequently, the centrocrista appears broadly V-shaped in occlusal view. The postmetacrista is weak or undeveloped on all P4s at hand. The lingual part of the crown consists of a low protocone and expansive talon. Although the base of the protocone is nearly as expansive as that of the paracone, the cusp is lower, approximately one-half to two-thirds the height of the paracone, and is situated far anteriorly on the crown, with the apex positioned at (e.g., TMP 2017.025.0452; Fig. 4.16) or slightly anterior to (e.g., TMP 2018.014.0276) the level of that of the paracone; the positions of the paracone and protocone result in a weakly excavated anterior margin, forming a shallow preflexus (sensu Hooker and Russell, 2012). A conspicuous preprotocrista extends labially from the protocone apex, terminating at the level of the paraconule just lingual and slightly anterior to the base of the paracone. The paraconule consists of only a short postparaconule crista and a longer preparaconule crista that continues anterolabially as the paracingulum. A metaconule is not present. The postprotocrista is undeveloped, with the posterior and posterolingual margin of the crown composed solely of the heavy postprotocone fold + posterior cingulum enclosing a shallow, posteriorly sloping talon basin. The postprotocone fold + posterior cingulum extends a short distance posteriorly, or posterolingually, and dorsally from the apex of the protocone before curving labially toward the metastylar corner of the crown; a result of this arrangement is that the posterolingual parts of the crown are significantly dorsal to the level of the more anterior parts. A hypocone is not developed. The anterior cingulum is uniformly short, terminating at the level of the paraconule, but it can vary in its conspicuousness: on some specimens (e.g., TMP 2018.014.0276), the anterior cingulum is only weakly developed, whereas in others (e.g., TMP 2017.025.0452) it can be stronger and anteriorly protruding.

M1.—The M1 of *Ignacius glenbowensis* n. sp. is known from two specimens that include other teeth (the holotype, TMP 2017.025.0452, and UALVP 60942) as well as several isolated teeth. The crown is subrectangular in occlusal outline, with the labial margin subequal to or slightly longer than the lingual margin. The labial side of the crown consists of a large, subconical paracone and slightly smaller and lower metacone. The stylar shelf is generally narrow, but variably developed: in several specimens (e.g., UALVP 60942; Fig. 4.19), the shelf is scarcely developed, and the labial margin of the crown consists only of the thick ectocingulum, whereas in other specimens (e.g., TMP 2017.025.0452; Fig. 4.16), the shelf is better developed anteriorly and posteriorly, and a weak ectoflexus is accordingly present, dividing the labial margin into distinct anterior and posterior parts. The preparacrista is short, extending anteriorly from the paracone apex where it meets the paracingulum + ectocingulum. The postparacrista and premetacrista are steep and deflected slightly lingually, and the notch in the centrocrista is deep. A weak postmetacrista occurs on some specimens (e.g., UALVP 60942; Fig. 4.19), whereas in others (e.g., TMP 2017.025.0454; Fig. 5.5) it is stronger. Although a distinct paraconule is not present, a strong inflection of the enamel at the junction of the preparaconule and postparaconule crista, just lingual and anterior to the base of the paracone, suggests its presence; the preparaconule crista continues anteriorly and labially as the paracingulum. As with the paraconule, a distinct metaconule is not developed; the premetaconule crista is usually continuous with the postprotocrista and often extends toward the apex of the metacone, whereas the postmetaconule crista is very weak or undeveloped. The anteriorly positioned protocone is slightly lower than the paracone, is more anteroposteriorly compressed, and its apex leans anteriorly. A robust preprotocrista runs labially and slightly anteriorly toward the paracone, joining the paraconule cristae + paracingulum. The postprotocrista becomes more conspicuous as it progresses posterolabially from the protocone apex, becoming stronger as it nears the metacone, where it can ascend the lingual side of that cusp before fading away. The postprotocone fold + postcingulum sweeps posteriorly and lingually before turning abruptly labially to enclose a shallow talon basin, which can be shorter (e.g., TMP 2017.025.0454; Fig. 5.5) or longer (e.g., TMP 2013.011.0016; Fig. 5.10) but is shallow in all cases, and the posterolingual parts of the crown are significantly dorsal to the level of the more anterior parts. The postprotocone fold + postcingulum continues uninterrupted to the metastylar corner of the crown. The lingual sides of the protocone and talon can be separated by a shallow groove, imparting a mildly bilobed appearance to that part of the crown (e.g., TMP 2013.011.0016; Fig. 5.6–5.10; TMP 2017.025.0454; Fig. 5.1–5.5), or these can be more swollen, obscuring the groove and presenting a flat to slightly convex surface (e.g., UALVP 60942; Figs. 4.18, 4.19). A hypocone is not developed. The anterior cingulum is robust, forming a shelf-like structure that extends from just dorsal of the protocone apex to the level of the paraconule.

M2.—The M1 and M2 of *Ignacius glenbowensis* n. sp. are similar in morphology, and accordingly can be difficult to distinguish from one another. The M2 is on average anteroposteriorly shorter but slightly wider than M1 (although the overlap in both length and width is extensive) (Table 2), and the crown is often skewed such that the paracone and metacone are oriented at more of an oblique angle to the long axis of the tooth row; as a result, the paracone and parastylar lobe tend to project farther labially, and the anterior margin of the crown is gently convex (e.g., TMP 2017.025.0452; Fig. 4.16). As with M1, the ectoflexus is variably developed in M2, with some specimens (e.g., TMP 2013.011.0349; Fig. 5.20) having a weakly concave labial margin, and others (e.g., UALVP 60942; Fig. 4.19) having no ectoflexus at all. The M2 differs further from M1 in the following

https://doi.org/10.1017/jpa.2022.103 Published online by Cambridge University Press

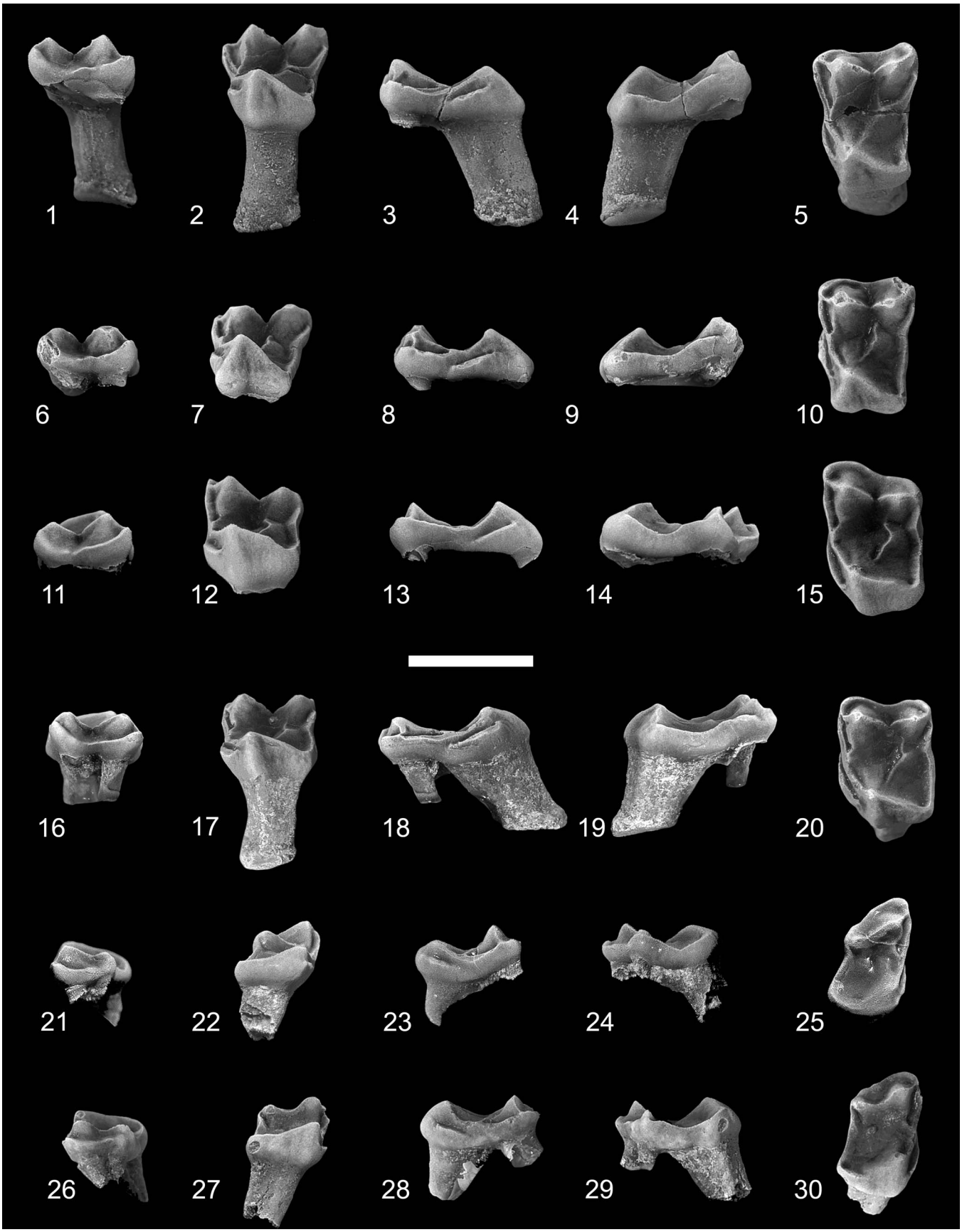

https://doi.org/10.1017/jpa.2022.103 Published online by Cambridge University Press

Figure 5. *Ignacius glenbowensis* n. sp. from the Paskapoo Formation, late Paleocene, southwestern Alberta. (**1–5**) TMP 2017.025.0454 (TS), LM1: (**1**) labial view; (**2**) lingual view; (**3**) anterior view; (**4**) posterior view; (**5**) occlusal view. (**6–10**) TMP 2013.011.0016 (C1), LM1: (**6**) labial view; (**7**) lingual view; (**8**) anterior, view; (**9**) posterior view; (**10**) occlusal view. (**11–15**) TMP 2013.048.0163 (TS), LM2: (**11**) labial view; (**12**) lingual view; (**13**) anterior view; (**14**) posterior view; (**15**) occlusal view. (**16–20**) TMP 2013.011.0349 (C1), LM2: (**16**) labial view; (**17**) lingual view; (**18**) anterior view; (**19**) posterior view; (**20**) occlusal view. (**21–25**) UALVP 24823 (C2), RM3: (**21**) labial view; (**22**) lingual view; (**23**) anterior view; (**24**) posterior view; (**25**) occlusal view. (**26–30**) TMP 2013.048.0059 (TS), RM3: (**26**) labial view; (**27**) lingual view; (**28**) anterior view; (**29**) posterior view; (**30**) occlusal view. TS = Trainspotting locality; C1 = Cochrane 1 locality; C2 = Cochrane 2 locality. Scale bar = 2 mm.

ways: the preparacrista generally curves anteriorly and labially (as opposed to extending directly anteriorly), and the parastylar lobe is often more drawn out in M2; the postmetacrista is shorter and more arcuate, curving a short distance posterolabially before joining the ectocingulum; and the talon is generally more extensive on M2, being longer and sometimes more lingually expansive.

M3.—The crown of M3 is roughly subquadrate in occlusal view, but distinctly asymmetrical, with subparallel anterior and posterior sides, and oblique labial and lingual margins. The labial side of the crown is dominated by a large subconical paracone and a smaller and lower metacone; the metacone is positioned posterior and lingual to the level of the paracone, resulting in the labial margin of the crown being oriented anterolabially-posterolingually. The parastylar lobe projects anterolabially, strongly in some specimens (e.g., UALVP 24823; Fig. 5.25) and more weakly in others (e.g., TMP 2013.048.0059; Fig. 5.30). The stylar shelf is otherwise undeveloped, and the labial margin of the crown consists only of the heavy ectocingulum. The preparacrista is short, directed anterolabially, joining the ectocingulum + paracingulum. The centrocrista is widely notched, with the postparacrista being significantly longer than the premetacrista. The postmetacrista is not present. As with M1 and M2, a distinct paraconule is not present on M3, although both preparconule and postparaconule cristae are conspicuous. The metaconule and metaconule cristae are absent. The protocone is both smaller and lower than the paracone, anteriorly positioned, and its apex leans anteriorly. The preprotocrista extends labially, joining the paracingulum, whereas the postprotocrista is undeveloped, and the posterior side of the protocone grades imperceptibly into the broad talon basin. The postprotocone fold + postcingulum extends posteriorly and slightly lingually before turning labially, enclosing a shallow talon basin that can extend posteriorly well past the level of the metacone (e.g., UALVP 24823; Fig. 5.25). The postprotocone fold + postcingulum continues uninterrupted to the metastylar corner of the crown.

p4.—The p4 of *Ignacius glenbowensis* n. sp. is represented by 12 specimens. Like that of other species of *Ignacius*, the crown consists of a short, swollen protoconid and a simple, shallow talonid, and appears wedge-shaped in occlusal outline (Fig. 6). The protoconid is strongly convex on its anterior, labial, and lingual walls; the postvallid wall is flat and steeply inclined. Neither paraconid, paracristid, nor metaconid is developed. A pair of crests, one labial and one lingual, descend posteriorly from the protoconid apex; the labial crest joins the cristid obliqua, whereas the lingual crest terminates just anterior to the entoconid, leaving the talonid open lingually. The talonid consists of a subequal hypoconid and entoconid; the two cusps are joined by a posteriorly convex crest that forms the posterior margin of the crown. A hypoconulid is not developed. The talonid basin is shallow and weakly concave. Neither a precingulid nor postcingulid is present.

m1.—The m1 of *Ignacius glenbowensis* n. sp. is low crowned, with a short, anteriorly leaning trigonid and a wide talonid. The crown is subtrapezoidal in occlusal outline, with the talonid significantly wider than the trigonid. A massive metaconid dominates the trigonid, followed by a subequal to slightly smaller and lower protoconid, and a subconical paraconid. The paraconid occurs just labial to the lingual margin of the crown and is appressed to the metaconid. The paracristid extends labially from the paraconid apex before turning sharply posteriorly to ascend the anterior wall of the protoconid and enclosing a low shallow trigonid basin. The protoconid and metaconid are joined by a high, sharp protocristid; the metaconid is positioned slightly posterior to the level of the protoconid, and the protocristid is aligned anterolabially-posterolingually. Unlike the m1 of *Edworthia*, the protocristid on m1 of *I. glenbowensis* is unnotched. The talonid basin is wider than long, shallow, and slopes lingually, with its deepest point occurring just labial to the talonid notch. In some specimens (e.g., UALVP 60951; Fig. 6.9), the talonid is only slightly wider than the trigonid, whereas in others (e.g., UALVP 24830; Fig. 7.4) it is considerably wider. The talonid cusps consist primarily of a low, posterolabially positioned hypoconid and a taller entoconid. The hypoconulid is variably developed: when present (e.g., UALVP 24830; Fig. 7.4), it is displaced labially from the midline, occurring as a weak bulge of enamel immediately lingual to the hypoconid; accordingly, the posterior margin of the crown is formed by an elongate, weakly convex postcristid and a short hypocristid. The cristid obliqua meets the postvallid wall slightly labial to the anteroposterior midline and can continue towards the apex of the metaconid (e.g., UALVP 24830; Fig. 7.3) or quickly fade away (e.g., UALVP 60961; Fig. 7.7). The entocristid is short and low, and the talonid notch is relatively shallow. The ectocingulid is usually undeveloped, but in several specimens (e.g., UALVP 24803), it is confined to a short shelf below the hypoflexid.

m2.—The crown of m2 (Fig. 7.9–7.16) resembles that of m1, differing mainly in its larger size, wider trigonid and talonid, and in having a lower trigonid relative to the talonid. The trigonid of m2 is more anteroposteriorly compressed than on m1, and the trigonid basin is accordingly shorter. The paracristid and protocristid are longer, the paraconid is smaller, situated more lingually, and more closely appressed to the metaconid, and the metaconid is less massive than on m1. The talonid is nearer in width to the trigonid, although like that on m1, the entoconid is positioned well lingual to the level of the metaconid. In addition to being considerably longer and wider, the talonid on m2 is shallower than on m1, the entoconid is relatively and absolutely larger, the hypoconid is lower, and the cristid obliqua contacts the postvallid wall farther labially. As on m1,

https://doi.org/10.1017/jpa.2022.103 Published online by Cambridge University Press

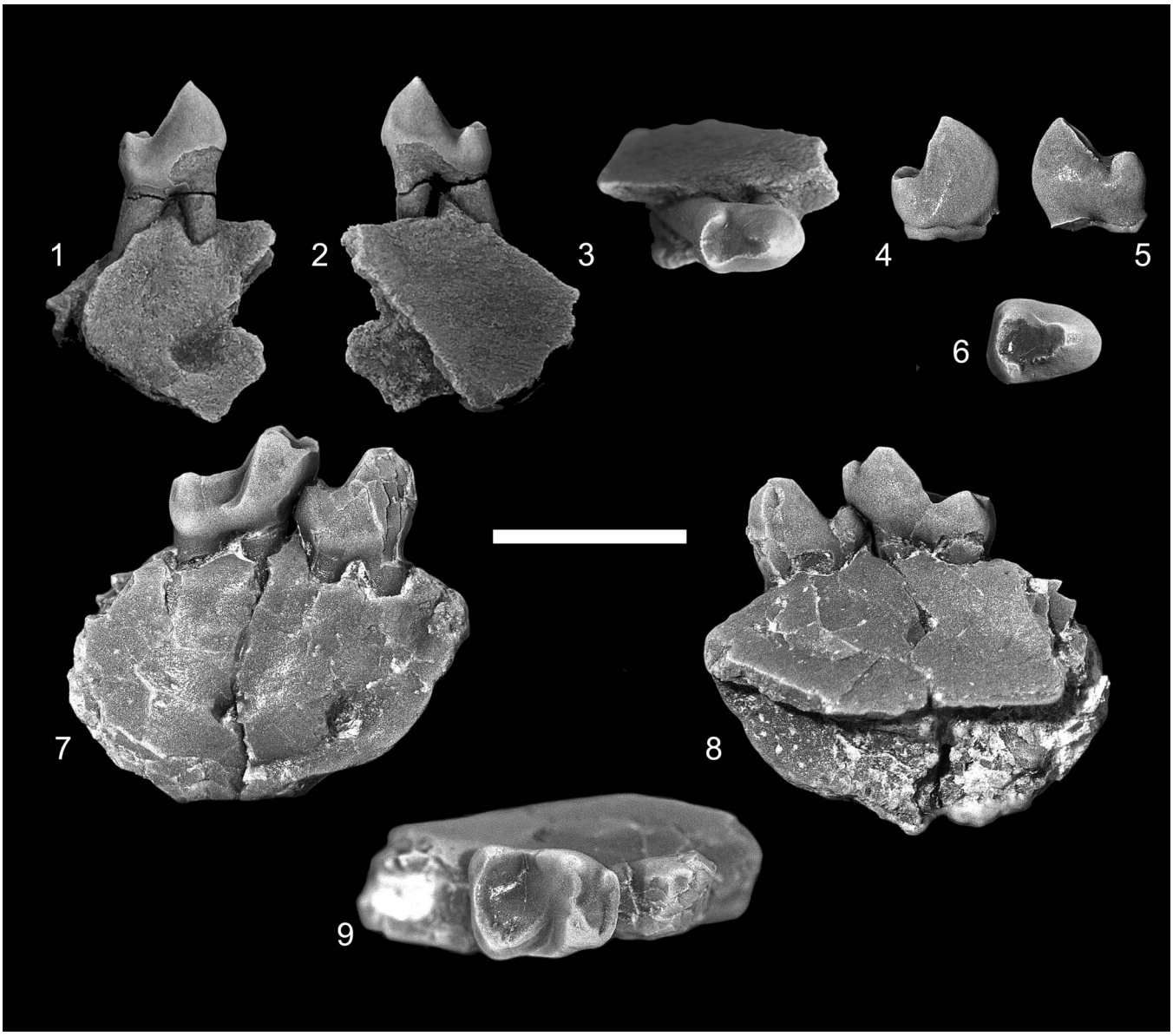

Figure 6. *Ignacius glenbowensis* n. sp. from the Paskapoo Formation, late Paleocene, southwestern Alberta. (**1–3**) TMP 2015.069.1106 (TS), incomplete right dentary with p4: (**1**) labial view; (**2**) lingual view; (**3**) occlusal view. (**4–6**) UALVP 60952 (C2), Rp4: (**4**) labial view; (**5**) lingual view; (**6**) occlusal view. (**7–9**) UALVP 60951 (C2), incomplete right dentary with p4, m1: (**7**) labial view; (**8**) lingual view; (**9**) occlusal view. TS = Trainspotting locality; C2 = Cochrane 2 locality. Scale bar = 2 mm.

the ectocingulid on m2, when present, is restricted to a robust shelf just below the hypoflexid.

m3.—The crown of m3 (Fig. 7.17–7.28) is substantially longer than that of m1 or m2, but narrower, particularly the talonid. The trigonid is more anteroposteriorly compressed than on m2, and the metaconid is much smaller, being subequal to the paraconid (which itself is smaller than that on m2). The conical paraconid occurs just labial to the lingual margin of the crown and is appressed to the metaconid; the shelf-like paracristid extends labially from the paraconid apex before turning sharply posteriorly, joining the protoconid and enclosing an anteroposteriorly compressed trigonid basin. The protoconid is the lowest trigonid cusp and is positioned anterior to the level of the metaconid; as a result, the protocristid extends posterolingually from the protoconid apex, and the protocristid is unnotched. The talonid basin is significantly longer than wide, varying from two and a half to three times the length of the trigonid, shallow, and slopes lingually, with its deepest point occurring just labial to the talonid notch. The hypoconid is low but massive, occupying a significant part of the labial side of the talonid. The subconical entoconid occurs slightly posterior to the level of the hypoconid and is separated from the postvallid wall by a narrow trigonid notch; an entocristid is not developed. The most conspicuous feature of the talonid is the greatly enlarged posterior lobe, which can be nearly as wide as the remainder of the talonid (e.g., UALVP 60972; Fig. 7.24) or significantly narrower (e.g., TMP 2015.069.0786; Fig. 7.28). The lobe is weakly subdivided posteriorly at the midline by a shallow fissure, producing a lingual lobe supporting a small cusp and a labial lobe supporting a lower and more massive cusp. Wear is usually strong on the

https://doi.org/10.1017/jpa.2022.103 Published online by Cambridge University Press

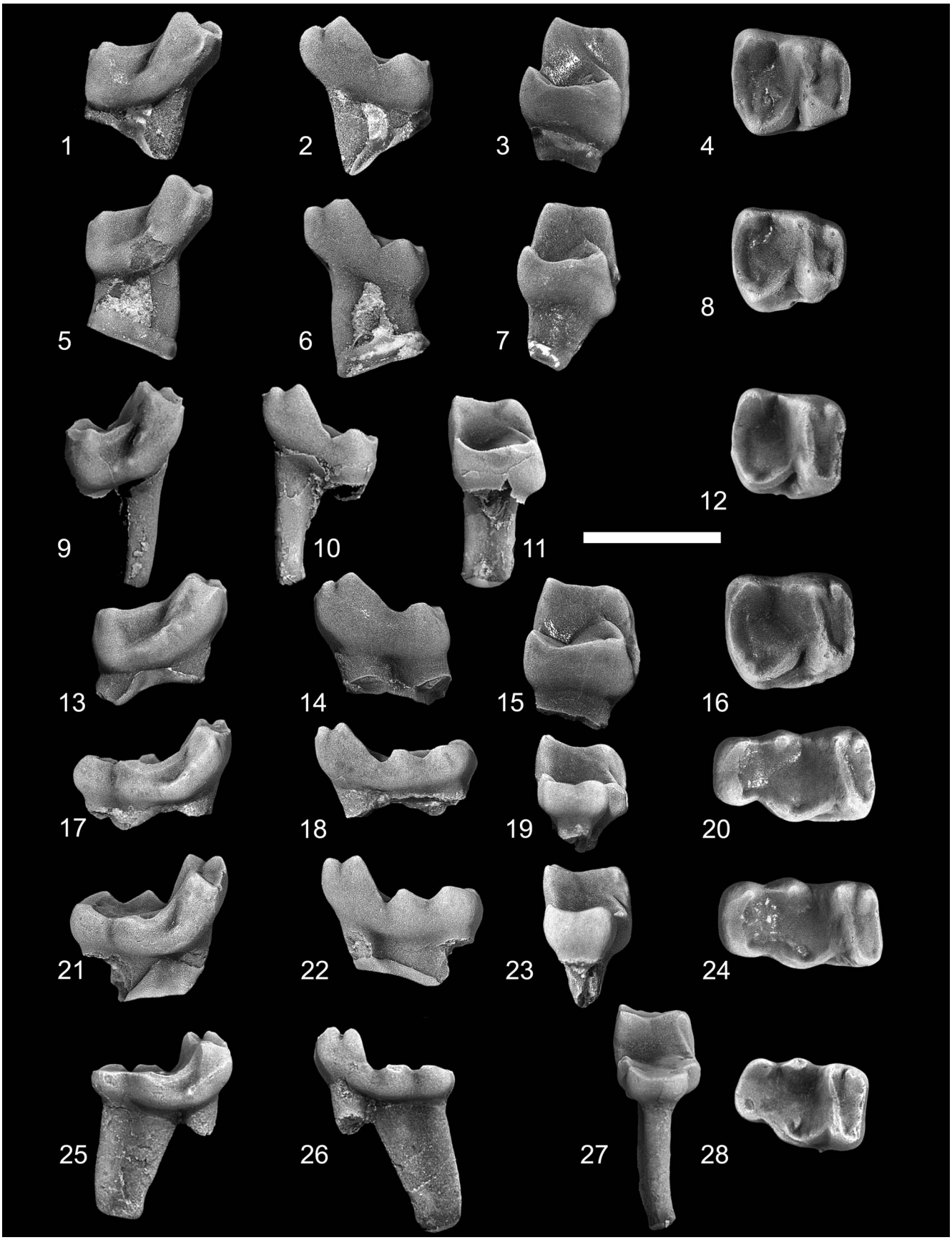

https://doi.org/10.1017/jpa.2022.103 Published online by Cambridge University Press

Figure 7. *Ignacius glenbowensis* n. sp. from the Paskapoo Formation, late Paleocene, southwestern Alberta. (**1–4**) UALVP 24830 (C2), Rm1: (**1**) labial view; (**2**) lingual view; (**3**) posterior view; (**4**) occlusal view. (**5–8**) UALVP 60961 (C2), Rm1: (**5**) labial view; (**6**) lingual view; (**7**) posterior view; (**8**) occlusal view. (**9–12**) TMP 2015.069.0013 (TS), Lm2: (**9**) labial view; (**10**) lingual view; (**11**) posterior view; (**12**) occlusal view (all views reversed from original). (**13–16**) UALVP 24836 (C2), Rm2: (**13**) labial view; (**14**) lingual view; (**15**) posterior view; (**16**) occlusal view. (**17–20**) UALVP 60973 (C2), Rm3: (**17**) labial view; (**18**) lingual view; (**19**) posterior view; (**20**) occlusal view. (**21–24**) UALVP 60972 (C2), Rm3: (**21**) labial view; (**22**) lingual view; (**23**) posterior view; (**24**) occlusal view. (**25–28**) TMP 2015.069.0786 (TS), Lm3: (**25**) labial view; (**26**) lingual view; (**27**) posterior view; (**28**) occlusal view (all views reversed from original). TS = Trainspotting locality; C2 = Cochrane 2 locality. Scale bar = 2 mm.

posterior lobe, blunting the cusps and producing a pair of transversely opposed facets connected by a crest. A broadly notched postcristid connects the lingual cusp to the entoconid, whereas the hypocristid extends anteriorly and labially, connecting the labial cusp to the hypoconid. The cristid obliqua meets the postvallid wall in a labial position, and the ectocingulid is confined to a short shelf below the hypoflexid.

Etymology.—In reference to Glenbow Ranch Provincial Park in southwestern Alberta, where the type locality occurs.

Materials.—

From Cochrane 1.—TMP 2017.035.0052, I1; TMP 2013.011.0016, 2015.070.0081, M1; TMP 2013.011.0349, 2014.023.0086, M2; TMP 2013.011.0480, p4; TMP 2011.108.0002, m1; TMP 2013.011.0449, m2; TMP 2013.011.0494, m3.

From Trainspotting.—TMP 2016.039.0036, 2016.039.0056, I1; TMP 2015.069.0136, 2016.039.0173, 2018.014.0276, P4; TMP 2013.048.0103, incomplete P4; TMP 2015.069.0832, 2017.025.0453, 2017.025.0454, M1; TMP 2013.048.0163, 2018.014.0199, M2; TMP 2015.069.0403, 2015.069.0307, M1 or M2; TMP 2014.047.0107, 2017.025.0178, 2017.025.0451, incomplete M1 or M2; TMP 2013.048.0059, 2018.014.0228, M3; TMP 2015.069.1106, incomplete dentary with p4; TMP 2017.025.0455, p4; TMP 2012.027.0004, 2016.039.0153, m1; TMP 2015.069.0013, 2015.069.0680, 2018.014.0188, 2018.014.0216, m2; TMP 2017.025.0435, m1 or m2; TMP 2015.069.0786, 2016.039.0034, m3.

From Cochrane 2.—UALVP 11744, 24811, 24818, 24824, 24837, 60936, 60937, 60938, 60939, P4; UALVP 24829, 60940, 60941, incomplete P4; UALVP 60942, incomplete maxilla with M1–2; UALVP 24802, 60943, 60944, 60945, 60946, M1; UALVP 24844, incomplete M1; UALVP 24804, 60947, 60948, M2; UALVP 18464, 24812, incomplete M2; UALVP 24834, incomplete M1 or M2; UALVP 18368, 24800, 24823, 60949, 60950, M3; UALVP 24848, incomplete M3; UALVP 60951, incomplete dentary with p4, m1; UALVP 11752, 24809, 24810, 24813, 24827, 60952, 60953, 60954, 60955, 60956, 60957, 60958, p4; UALVP 24803, 24847, 24830, 24831, 24845, 60959, 60960, 60961, 60962, 60963, 60964, m1; UALVP 24833, 60965, incomplete m1; UALVP 24835, 24836, 24849, 60966, 60967, 60968, 60969, 60970, m2; UALVP 24838, 24842, incomplete m2; UALVP 24832, 60971, 60972, 60973, 60974, 60975, 60976, 60977, m3; UALVP 24816, 24817, 24846, 60978, incomplete m3.

Table 2. Combined measurements and descriptive statistics for the dentition of *Ignacius glenbowensis* n. sp. from the Paskapoo Formation of southwestern Alberta, Canada. P = parameter; N = number; OR = observed range; MN = mean; SD = standard deviation; CV = coefficient of variation; P/p = upper/lower premolar; M/m = upper/lower molar; L = anteroposterior length; W = maximum crown width. Individual specimen measurements in Supplemental Data 3.

Element	P	N	OR	MN	SD	CV
P4	L	11	1.53–1.83	1.69	0.088	0.052
	W	10	1.95–2.14	2.03	0.062	0.030
M1	L	11	1.62–2.02	1.84	0.110	0.061
	W	10	2.30–2.72	2.56	0.120	0.049
M2	L	8	1.59–1.85	1.71	0.079	0.046
	W	8	2.56–2.82	2.74	0.080	0.029
M3	L	6	1.36–1.68	1.45	0.160	0.110
	W	6	2.17–2.50	2.29	0.120	0.051
p4	L	12	1.31–1.70	1.47	0.120	0.083
	W	12	0.90–1.17	1.02	0.085	0.083
m1	L	14	1.63–1.98	1.83	0.100	0.055
	W	13	1.30–1.55	1.43	0.078	0.054
m2	L	11	1.65–1.89	1.80	0.081	0.045
	W	11	1.38–1.61	1.47	0.066	0.045
m3	L	7	2.20–2.47	2.34	0.083	0.036
	W	7	1.25–1.40	1.33	0.064	0.048

Remarks.—In his study of the mammals from the Cochrane 2 locality, Youzwyshyn (1988) referred several specimens to two species of *Ignacius*, *I. fremontensis* and *Ignacius* cf. *I. frugivorus*, but noted several differences that distinguished these specimens from *I. fremontensis* and *I. frugivorus* (e.g., slightly larger size of the teeth referred to *I. fremontensis* and the more transverse molars and poorly developed molar talon in the specimens referred to *I. frugivorus*). We can confirm these differences, both in the Cochrane 2 sample and in those from Trainspotting and Cochrane 1, and consider these to be of taxonomic significance; we accordingly refer these samples to a new species, *I. glenbowensis* n. sp.

Intersample comparison.—Although *Ignacius glenbowensis* n. sp. is known from the earliest Tiffanian (Ti1), the localities at which it occurs represent time horizons very early (Cochrane 1, Trainspotting, both near the base of magnetochron 26r; localities projected onto the stratigraphic framework presented in Lerbekmo and Sweet, 2000, and see Scott et al., 2013) and significantly later (Cochrane 2, occurring some 100 m higher and hence later in 26r; Russell, 1929) in the biozone. Subtle differences in several features between the Cochrane 1/Trainspotting samples and that from Cochrane 2 are noted. For example, when compared with the Cochrane 1/Trainspotting sample, several of the P4s from Cochrane 2 have a stronger ectocingulum that extends to the metacone (and sometimes toward the cusp apex), the metacone is generally smaller, and the hypoconal shelf is better developed, extending farther lingually and forming a more distinct lobe. The M1 and M2, while nearly identical in most features between samples, differ in those from Cochrane 1 and Trainspotting having a slightly deeper ectoflexus, particularly on M2. The M3 is highly variable in the Cochrane 2 sample, but it differs in general from those from Trainspotting in having a slightly smaller metacone. The p4 is generally larger and more swollen, and the talonid tends to be slightly wider (resulting in a more distinctly wedge-shaped

https://doi.org/10.1017/jpa.2022.103 Published online by Cambridge University Press

occlusal outline) in the Cochrane 2 sample, and the m3 is slightly larger. The meaning of these differences is difficult to interpret. Although the differences seen in the Cochrane 2 sample may suggest the presence of a species separate from that of *I. glenbowensis*, the variation within the Cochrane 2 sample itself—which in some cases encompasses the morphology in the smaller sample sizes from Cochrane 1 and Trainspotting—is great, suggesting a variable but single species. The kind and degree of variation seen in the Alberta samples is largely congruent with that documented for other paromomyids (e.g., the development of the paraconid on the m2 in *Ignacius graybullianus* [Silcox et al., 2008], the degree of fissuring of the m3 hypoconulid lobe in *Phenacolemur praecox* [Silcox et al., 2008]), and for plesiadapiforms more generally (e.g., the size of the I1 mediocone in the plesiadapid *Pronothodectes matthewi*, the presence/absence of the metacone on P3 and P4 of various species of the plesiadapid *Nannodectes*, and the variable presence of p2 in the plesiadapid *Plesiadapis churchilli* [Gingerich, 1976], as well as the size of the mediobasal cusp on I1 of the carpolestid *Carpodaptes cygneus* [Fox, 2002]). Until larger samples can be obtained from both Cochrane 1 and Trainspotting, we provisionally consider *I. glenbowensis* to be the sole species of *Ignacius* represented at these earliest Tiffanian localities.

Comparisons with other species of *Ignacius*.—*I. glenbowensis* n. sp. resembles *I. fremontensis* and *I. frugivorus* most closely among species of the genus. When compared with *I. fremontensis*, the teeth of *I. glenbowensis* are slightly larger in linear dimensions, particularly crown width (e.g., width m1 = 1.2 in *I. fremontensis* versus mean width m1 = 1.43 in *I. glenbowensis*; Gazin, 1971); the stylar shelf on M1 and M2 is generally narrower (although as noted earlier, the ectoflexus is variable in its development, and on some specimens more closely resembles the condition in *I. fremontensis*; see Szalay and Delson, 1979); the talon is better developed, extending both farther lingually and posteriorly (in some specimens, especially those from Cochrane 2, the talon is somewhat inflated lingually, and the lingual wall of the protocone is only weakly bilobate); and the molar protocone cristae are weaker, and the paraconule is generally more poorly developed. The few specimens that preserve parts of the dentary anterior to p4 suggest that p3 is not developed in *I. glenbowensis*, although the sample size is too small to assess possible variation in the presence of this tooth (note, e.g., the variable presence of p2 in the plesiadapid *Plesiadapis churchilli*; Gingerich, 1976). The p4 of *I. glenbowensis* is on average slightly larger relative to m1 when compared with that of *I. fremontensis*. The molar paraconid is more lingual and relatively smaller in *I. glenbowensis*, the talonid on m1 and m2 is both wider relative to the trigonid and anteroposteriorly shorter, the hypoflexid shelf is more prominent, and the hypoconulid lobe is better differentiated on m3. When compared with *I. frugivorus*, the teeth of *I. glenbowensis* are smaller overall (e.g., compare with measurements in Krause, 1978, table 7), the P4 has a much weaker parastylar lobe and metacone, the talon is more poorly developed, and the crown retains a somewhat rectangular outline (in *I. frugivorus*, the P4 has become nearly square in outline owing to the great expansion of the talon; see Simpson, 1955; Krause, 1978). The stylar shelf on M1 and M2 is wider and the ectoflexus more pronounced (in at least some specimens), and the crowns are more rectangular in outline in *I. glenbowensis* (compare with the M1 and M2 in *I. frugivorus*, where the M1 is essentially square in outline, owing to an anteroposteriorly expanded protocone and the talon extending posteriorly and lingually; Simpson, 1955; Krause, 1978). The molar paracone and metacone are more closely appressed in *I. glenbowensis* (and the centrocrista notch is accordingly deeper and more acute), and the lingual wall of upper molars is less inflated, resulting in a moderately bilobate appearance. The m1 and m2 talonid is less expanded posteriorly and lingually in *I. glenbowensis*, in keeping with the more compressed protocone and more weakly expanded talon, the m2 paraconid is more lingual, and the molar cristid obliqua contacts postvallid wall slightly more lingually.

Analysis

Systematic positions of Edworthia greggi *n. sp. and* Ignacius glenbowensis *n. sp.*—The cladistic analysis retained 264 most parsimonious trees, and from these an Adams consensus (Fig. 8.1, Supplemental Figure 1) and a strict consensus tree were generated (Fig. 8.2). The Adams tree has *Paromomys* recovered as the most basal paromomyid, and the palaechthonids *Premnoides* and *Torrejonia* appear as the most closely related taxa to paromomyids in our sample. *Paromomys* was recovered as a paraphyletic genus, with *Pa. depressidens* recovered as the species of *Paromomys* most closely related to the non-*Paromomys* paromomyids, and the remaining species recovered at successively more stemward positions. *Edworthia* was recovered immediately crownward of several species of *Paromomys*, in a polytomy with *Pa. depressidens*. *Ignacius* is also paraphyletic, with *I. graybullianus* and *I. clarkforkensis* being sister taxa and occupying the basalmost position within the genus. *Ignacius frugivorus*, *I. glenbowensis*, and *I. fremontensis* appear at successively crownward positions, with *I. fremontensis* being the sister group of the *Acidomomys–Phenacolmeur–Elwynella–Arcius* clade. Although all nodes outside of the paromomyid clade are stable and hold equivalent positions in both consensus trees, node instability characterizes the strict consensus tree. *Paromomys maturus* appears as the sister taxon to the rest of the paromomyids in both trees, but the remaining paromomyids form a large polytomy in the strict consensus tree, in which only a few clades were recovered, including the *Phenacolemur praecox–fortior* clade, the *Ignacius graybullianus–clarkforkensis* clade, and the clade that includes *Arcius*, *Elwynella*, *Phenacolemur jepseni* Simpson, 1955, and *Phenacolemur willwoodensis* Silcox, Rose, and Bown, 2008. The relationships among species of *Arcius* are not resolved in the strict consensus tree, although the genus was nonetheless recovered as monophyletic. The contrast between the two trees reflects the fact that several relatively poorly known species (e.g., *Pa. farrandi*, *Pa. libedianus*) likely act as wildcard taxa, occupying a range of positions on the various equally parsimonious trees. The Adams tree preserves the structure that remains when such taxa occur, at the highest node at which their position can be resolved.

An unexpected result attends *Foxomomys* and *Navajovius*, recovered here in a position basal to that of *Purgatorius*. Micromomyids have generally been hypothesized to be among the most basal plesiadapiforms in previous phylogenetic analyses

https://doi.org/10.1017/jpa.2022.103 Published online by Cambridge University Press

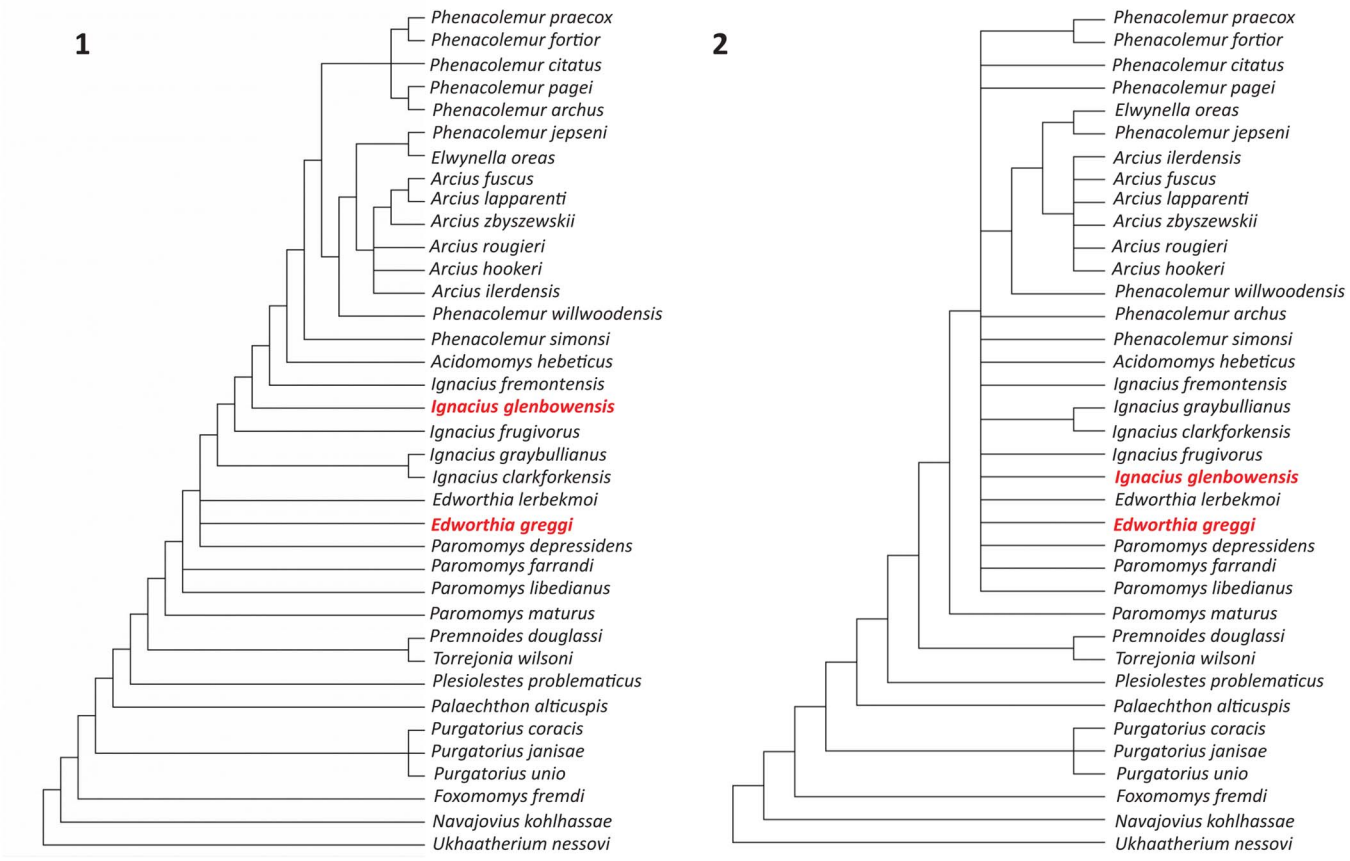

Figure 8. Hypothesized phylogenetic relationships of *Edworthia greggi* n. sp. and *Ignacius glenbowensis* n. sp. (highlighted in red font) from the Paleocene Paskapoo Formation, southwestern Alberta. (**1, 2**) Consensuses of 164 most parsimonious trees: (**1**) Adams consensus; (**2**) strict consensus.

(Silcox, 2001; Bloch et al., 2007; Silcox et al., 2010), and more recently, the results of the analysis conducted by Chester et al. (2015) found a sister group relationship between *Foxomomys* and *Purgatorius* (rather than grouping *Foxomomys* with other micromomyids included in that analysis). Given these contrasting results, it seems apparent that the phylogenetic position of *Foxomomys* relative to other plesiadapiforms is not well understood and may be particularly sensitive to taxon and character choice, as well as tree-searching methods. Similar to micromomyids, microsyopids have also been recovered previously as one of the most basal groups of plesiadapiforms (Silcox et al., 2020). While the results of several phylogenetic analyses support euarchontan affinities for microsyopids, their relationships within Euarchonta remain unclear (e.g., some authors have suggested a close relationship with Dermoptera [Szalay and Drawhorn, 1980; Szalay et al., 1987; Gunnell, 1989; Ni et al., 2013, 2016]), and these ongoing uncertainties are further reflected in the results of our analysis.

The dentitions of *E. greggi* n. sp. and *I. glenbowensis* n. sp. share several similarities with that of *Paromomys*, long considered the basalmost paromomyid so far discovered (Silcox, 2001; Silcox and Gunnell, 2008). While the results of our cladistic analysis suggest that many of these features are plesiomorphic for Paromomyidae, they nonetheless bolster previous hypotheses regarding the systematic positions of *Edworthia* and *Ignacius* and indicate that these taxa were among the earliest diverging members of the family (e.g., Fox et al., 2010). The newly discovered upper dentition of *Edworthia* reveals several important similarities with that of *Paromomys*; for example, both conules are present on M1–2, the lingual wall of the crown is cleft, imparting a bilobed appearance to that part of the crown (a feature that is variably present in *I. glenbowensis* and *I. fremontensis*), and the parastylar lobe on M3 is projecting, and the talon is not expanded posterolingually. Like those of *Paromomys*, the upper molars of *Edworthia* are rectangular in outline, owing primarily to the poorly developed (i.e., less lingually and posteriorly extensive) talon and anteroposteriorly compressed protocone, and the molar postparacrista and premetacrista are aligned anteroposteriorly, rather than deflected lingually, and the centrocrista is accordingly straighter and less V-shaped in occlusal view. By contrast, the upper molars of *Ignacius glenbowensis* are more squarish, with an inflated protocone and better developed talon, and the molar postparacrista and premetacrista are deflected somewhat lingually, resulting in a more V-shaped centrocrista. Several of these features are further developed in younger species of *Ignacius* and in *Phenacolemur*, where the upper molars are nearly square in outline, and the talons are greatly expanded posteriorly and lingually (Simpson, 1955; Krause, 1978; Silcox et al., 2008). Perhaps the most salient differences in the upper dentition of *Edworthia* and *Paromomys* concern the P4 and M3. In *Edworthia*, the P4 is smaller relative to M1 when compared with that of *Paromomys*,

https://doi.org/10.1017/jpa.2022.103 Published online by Cambridge University Press

and longer relative to width, resulting in a more squarish rather than rectangular outline. The M3 of *Edworthia* differs from that of *Paromomys* in having a stronger parastylar lobe and a smaller metacone and in being more hourglass-shaped in outline (rather than rectangular).

Conclusion

Paromomyids are the only plesiadapiforms that have been discovered in deposits at high latitudes (e.g., Ellesmere Island, Canadian Arctic; West and Dawson, 1977; Eberle and Greenwood, 2012), but the fossil record of this family—and other plesiadapiforms broadly–from more northerly geographic areas is relatively poorly known (e.g., Krause, 1978; Fox, 1991, 2011; MacDonald, 1996; Scott, 2008; Fox et al., 2010, 2014; Scott et al., 2013). Given this reality, the discovery of new species of two paromomyid genera from Alberta represents a welcome addition to the comparatively richer record from farther south. The newly discovered species of *Edworthia* and *Ignacius* document significant anatomical information for two comparatively poorly known paromomyid genera, and their occurrences in the middle Torrejonian and earliest Tiffanian provide snapshots of early paromomyid diversification during an important interval in the evolutionary history of primates. The specimens of *E. greggi* n. sp. provide the first anatomical information on the upper dentition of *Edworthia* and reveal important similarities with that of *Paromomys*, supporting earlier assertions—based on the lower dentition—that the genus is among the basalmost paromomyids so far discovered and represents the result of an early paromomyid divergence. Further, the sample of *I. glenbowensis* n. sp. from Alberta is among the largest known for the genus and provides not only important information on the dental morphology of the earliest stages of the *Ignacius* lineage, but a better understanding of intraspecific variation in an early paromomyid. The discovery of *E. greggi* and *I. glenbowensis* adds to what appears to be a uniquely Canadian assemblage of early primates, which includes not only regional species of geographically more widespread taxa (e.g., *Foxomomys fremdi* [Fox, 1984], *Pronothodectes gaoi* Fox, 1990, *Picrodus calgariensis* Scott and Fox, 2005) but those of genera that are presently known only from Alberta as well (e.g., *Edworthia*, *Phoxomylus* Fox, 2011). The discovery of these new species adds further documentation of a significant radiation of plesiadapiforms that began in the Torrejonian and continued well into the earliest parts of the late Paleocene.

Acknowledgments

We extend thanks to P. Holroyd and the late W. Clemens (University of California Museum of Paleontology), J. Eberle, T. Culver, and T. Karim (University of Colorado Boulder), M. Godinot and C. Argot (Muséum National d'Histoire Naturelle), R. Rocha (Universidade Nova de Lisboa), J. Hooker (British Museum of Natural History), J. Galkin, A. Davison, R. O'Leary, and J. Meng (American Museum of Natural History), P. Gingerich, W. Sanders, and A. Rountry (University of Michigan Museum of Paleontology), C. Norris, D. Brinkman, M. Fox, and E. Sargis (Yale Peabody Museum), D. Bohaska and N. Pyenson (National Museum of Natural History—Smithsonian Institution), K. Rose (The Johns Hopkins University), J. Bloch (Florida Museum of Natural History), T. Smith (Royal Belgian Museum of Natural Sciences), and G. Wilson Mantilla (University of Washington) for access to specimens in their respective institutions and/or casts, necessary for the phylogenetic analysis. Thanks to E. Charles, R. Bhagat, and D. Lin (University of Toronto Scarborough) for making relevant casts. We extend thanks to the late A. Voss (UALVP) for her efforts in sorting Cochrane 2 matrix and to G. Youzwyshyn, G. Stonley, K. Soehn (all UALVP), and L. Bohach (Stantec) for assistance in the field. Thanks are extended to Canadian Pacific Rail, and K. Sholes in particular, for continued access to the Trainspotting locality and to Alberta Culture and Status of Women and Alberta Environment and Parks for permission to excavate in Glenbow Ranch Provincial Park. We thank J. Calede, S. Chester, and two anonymous reviewers for comments that substantially improved this paper. This research was supported by the Doris O. and Samuel P. Welles Research Fund, an American Museum of Natural History Collections Study Grant, and a University of Toronto Department of Anthropology Research Travelling Grants to S.L.T. and an NSERC Discovery Grant to M.T.S.

Declaration of competing interests

The authors declare none.

Data availability statement

Data available from the Dryad Digital Repository: https://doi.org/10.5061/dryad.9p8cz8wkt and Zenodo Digital Repository: https://doi.org/10.5281/zenodo.7259030.

References

Aumont, A., 2004, Première découverte d'espèces sympatriques de Paromomyidés (Plesiadapiformes, Mammifères) en Europe: Comptes Rendus Palevol, v. 3, p. 27–34.

Beard, K.C., 1993, Phylogenetic systematics of the Primatomorpha, with special reference to Dermoptera, *in* Szalay, F.S., Novacek, M.J., and McKenna, M.C., eds., Mammal Phylogeny: Placentals: Springer-Verlag, New York, p. 129–150.

Bloch, J.I., and Silcox, M.T., 2001, New basicrania of Paleocene–Eocene *Ignacius*: re-evaluation of the plesiadapiform-dermopteran link: American Journal of Physical Anthropology, v. 116, p. 184–198.

Bloch, J.I., Boyer, D.M., Gingerich, P.D., and Gunnell, G.F., 2002, New primitive paromomyid from the Clarkforkian of Wyoming and dental eruption in Plesiadapiformes: Journal of Vertebrate Paleontology, v. 22, p. 366–379.

Bloch, J.I., Silcox, M.T., Boyer, D.M., and Sargis, E.J., 2007, New Paleocene skeletons and the relationship of plesiadapiforms to crown-clade primates: Proceedings of the National Academy of Sciences USA, v. 104, p. 1159–1164.

Bown, T.M., and Rose, K.D., 1976, New early Tertiary primates and a reappraisal of some Plesiadapiformes: Folia Primatologica, v. 26, p. 109–138.

Boyer, D.M., and Bloch, J.I., 2008, Evaluating the mitten-gliding hypothesis for Paromomyidae and Micromomyidae (Mammalia, "Plesiadapiformes") using comparative functional morphology of new Paleogene skeletons, *in* Sargis, E.J., and Dagosto, M., eds., Mammalian Evolutionary Morphology: A Tribute to Frederick S. Szalay: Springer, Dordrecht, p. 233–284.

Boyer, D.M., Chester, S.G.B., and Bloch, J.I., 2010, New fossil evidence on the plesiadapiform hand skeleton: implications for the evolution of grasping in primates: American Journal of Physical Anthropology, v. 140 (supplement), p. 72A.

https://doi.org/10.1017/jpa.2022.103 Published online by Cambridge University Press

Chester, S.G.B., and Bloch, J.I., 2013, Systematics of Paleogene Micromomyidae (Euarchonta, Primates) from North America: Journal of Human Evolution, v. 65, p. 109–142.
Chester, S.G.B., Bloch, J.I., Boyer, D.M., and Clemens, W.A., 2015, Oldest known euarchontan postcrania and affinities of Paleocene *Purgatorius* to Primates: Proceedings of the National Academy of Sciences USA, v. 112, p. 1487–1492.
Chester, S.G.B., Williamson, T.E., Bloch, J.I., Silcox, M.T., and Sargis, E.J., 2017, Oldest skeleton of a plesiadapiform provides additional evidence for an exclusively arboreal radiation of stem primates in the Palaeocene: Royal Society Open Science, v. 4, n. 170329, https://doi.org/10.1098/rsos.170329
Clemens, W.A., 1966, Fossil mammals of the type Lance Formation, Wyoming. Part II. Marsupialia: University of California Publications in Geological Sciences, v. 62, 122 p.
Clemens, W.A., and Wilson, G.P., 2009, Early Torrejonian mammalian local faunas from northeastern Montana, USA, *in* Albright, L.B., III, ed., Papers on Geology, Vertebrate Paleontology and Biostratigraphy in Honor of Michael O. Woodburne: Museum of Northern Arizona Bulletin, v. 65, p. 111–158.
Dawson, M.R., West, R.M., Langston, W., Jr., and Hutchison, J.H., 1976, Paleogene terrestrial vertebrates: northernmost occurrence, Ellesmere Island, Canada: Science, v. 192, p. 781–782.
Eberle, J.J., and Greenwood, D.R., 2012, Life at the top of the greenhouse Eocene world—a review of the Eocene flora and vertebrate fauna from Canada's High Arctic: Geological Society of America Bulletin, v. 124, p. 3–23.
Estravís, C., 2000, Nuevos mamíferos del Eoceno Inferior de Silveirinha (Baixo Mondego, Portugal): Coloquios de Paleontología, v. 51, p. 281–311.
Fox, R.C., 1984, The dentition and relationships of the Paleocene primate *Micromomys* Szalay, with description of a new species: Canadian Journal of Earth Sciences, v. 21, p. 1262–1267.
Fox, R.C., 1990, The succession of Paleocene mammals in western Canada, *in* Bown, T.M., and Rose, K.D., eds., Dawn of the Age of Mammals in the Northern Part of the Rocky Mountain Interior: Geological Society of America Special Papers, v. 243, p. 51–70.
Fox, R.C., 1991, *Saxonella* (Plesiadapiformes: ?Primates) in North America: *S. naylori*, sp. nov., from the late Paleocene of Alberta, Canada: Journal of Vertebrate Paleontology, v. 11, p. 635–657.
Fox, R.C., 2011, An unusual early primate from the Paleocene Paskapoo Formation, Alberta, Canada: Acta Palaeontologica Polonica, v. 56, p. 1–10.
Fox, R.C., Scott, C.S., and Rankin, B.D., 2010, *Edworthia lerbekmoi*, a new primitive paromomyid primate from the Torrejonian (early Paleocene) of Alberta, Canada: Journal of Paleontology, v. 84, p. 868–878.
Fox, R.C., Rankin, B.D., Scott, C.S., and Sweet, A.R., 2014, Second known occurrence of the early Paleocene plesiadapiform *Pandemonium* (Mammalia: Primates), with description of a new species: Canadian Journal of Earth Sciences, v. 51, p. 1059–1066.
Gazin, C.L., 1968, A new primate from the Torrejon middle Paleocene of the San Juan Basin, New Mexico: Proceedings of the Biological Society of Washington, v. 81, p. 629–634.
Gazin, C.L., 1971, Paleocene primates from the Shotgun Member of the Fort Union Formation in the Wind River Basin, Wyoming: Proceedings of the Biological Society of Washington, v. 84, p. 13–38.
Gidley, J.W., 1923, Paleocene primates of the Fort Union, with discussion of relationships of Eocene primates: Proceedings of the United States National Museum, v. 63, p. 1–38.
Gingerich, P.D., 1976, Cranial anatomy and evolution of early Tertiary Plesiadapidae (Mammalia, Primates): University of Michigan Papers on Paleontology, v. 15, 140 p.
Godinot, M., 1984, Un nouveau genre du Paromomyidae (Primates) de l'Eocène inférieur d'Europe: Folia Primatologica, v. 43, p. 84–96.
Godinot, M., Blondel, C., Escarguel, G., Lézin, C., Pélissié, T., Tabuce, R., Vidalenc, D., 2021, Primates and Plesiadapiformes from Cos (Eocene; Quercy, France): Geobios, v. 66–67, p. 153–176.
Gunnell, G.F., 1989, Evolutionary history of Microsyopoidea (Mammalia, ?Primates) and the relationship between Plesiadapiformes and Primates: University of Michigan Papers on Paleontology, v. 27, 157 p.
Hamblin, A.P., 2004, Paskapoo–Porcupine Hills formations in western Canada: synthesis of regional geology and resource potential: Geological Survey of Canada Open File 4679, 30 p.
Hoffstetter, R., 1977, Phylogénie des primates: Bulletins et mémoires de la Société d'anthropologie de Paris, v. 4, ser. 13, p. 327–346.
Hooker, J.J., and Russell, D.E., 2012, Early Palaeogene Louisinidae (Macroscelidea, Mammalia), their relationships and north European diversity: Zoological Journal of the Linnean Society, v. 164, p. 856–936.
Jepsen, G.L., 1930, New vertebrate fossils from the lower Eocene of the Bighorn Basin, Wyoming: Proceedings of the American Philosophical Society, v. 69, p. 117–131.
Jerzykiewicz, T., 1997, Stratigraphic framework of the uppermost Cretaceous to Paleocene strata of the Alberta Basin: Geological Survey of Canada Bulletin, v. 510, 20 p.
Kay, R.F., and Cartmill, M., 1977, Cranial morphology and adaptations of *Palaechthon nacimienti* and other Paromomyidae (Plesiadapoidea, ?Primates), with a description of a new genus and species: Journal of Human Evolution, v. 6, p. 19–53.
Kay, R.F., Thewissen, J.G.M., and Yoder, A.D., 1992, Cranial anatomy of *Ignacius graybullianus* and the affinities of the Plesiadapiformes: American Journal of Physical Anthropology, v. 89, p. 477–498.
Kihm, A.J., and Tornow, M.A., 2014, First occurrence of plesiadapiform primates from the Chadronian (latest Eocene): Paludicola, v. 9, p. 176–182.
Krause, D.W., 1978, Paleocene primates from western Canada: Canadian Journal of Earth Sciences, v. 15, p. 1250–1271.
Lerbekmo, J.F., and Sweet, A.R., 2000, Magnetostratigraphy and biostratigraphy of the continental Paleocene in the Calgary area, southwestern Alberta: Bulletin of Canadian Petroleum Geology, v. 48, p. 285–306.
Linnaeus, C., 1758, Systema naturae per regna tria naturae, secundum classes, ordines, genera, species cum characteribus, differentiis, synonymis, locis. Volume I: Regnum Animale. Editio decima, reformata: Stockholm, Laurenti Salvii. [facsimile reprinted in 1956 by the British Museum (Natural History)]
Lofgren, D.L., Lillegraven, J.A., Clemens, W.A., Gingerich, P.D., and Williamson, T.E., 2004, Paleocene biochronology: the Puercan through Clarkforkian Land Mammal Ages, *in* Woodburne, M.O., ed., Late Cretaceous and Cenozoic Mammals of North America: Geochronology and Biostratigraphy: New York, Columbia University Press, p. 43–105.
López-Torres, S., and Silcox, M.T., 2018, The European Paromomyidae (Primates, Mammalia): taxonomy, phylogeny, and biogeographic implications: Journal of Paleontology, v. 92, p. 920–937.
López-Torres, S., Silcox, M.T., and Holroyd, P.A., 2018, New omomyoids (Euprimates, Mammalia) from the late Uintan of southern California, USA, and the question of the extinction of the Paromomyidae (Plesiadapiformes, Primates): Palaeontologia Electronica 21.3.37A, https://doi.org/10.26879/756
MacDonald, T.E., 1996, Late Paleocene (Tiffanian) mammal-bearing localities in superposition, from near Drumheller, Alberta [M. Sc. Thesis]: Edmonton, University of Alberta, 248 p.
Matthew, W.D., 1915, A revision of the lower Eocene Wasatch and Wind River faunas. Entelonychia, Primates, Insectivora (part): Bulletin of the American Museum of Natural History, v. 34, p. 429–483.
Matthew, W.D., and Granger, W., 1921, New genera of Paleocene mammals: American Museum Novitates, no. 13, 13 p.
McKenna, M.C., 1980, Eocene paleolatitude, climate, and mammals of Ellesmere Island: Palaeogeography, Palaeoclimatology, Palaeoecology, v. 30, p. 349–362.
Miller, K., and Beard, K.C., 2020, Phylogenetic reconstruction of two species of paromomyid plesiadapiforms from a unique, High Arctic ecosystem of Eocene Canada: Journal of Vertebrate Paleontology, Program and Abstracts, 2020, p. 246.
Ni, X., Gebo, D.L, Dagosto, M., Meng, J., Tafforeau, P., Flynn, J.J., and Beard, K.C, 2013, The oldest known primate skeleton and early haplorhine evolution: Nature, v. 498, p. 60–64.
Ni, X., Li, Q., Li, L., and Beard, K.C, 2016, Oligocene primates from China reveal divergence between African and Asian primate evolution: Science, v. 352, p. 673–677.
Novacek, M.J., Rougier, G.W., Wible, J.R., McKenna, M.C., Dashzeveg, D., and Horowitz, I., 1997, Epipubic bones in eutherian mammals from the Late Cretaceous of Mongolia: Nature, v. 389, p. 483–486.
Robinson, P., and Ivy, L.D., 1994, Paromomyidae (?Dermoptera) from the Powder River Basin, Wyoming, and a discussion of microevolution in closely related species: Contributions to Geology, University of Wyoming, v. 30, p. 91–116.
Rose, K.D., 1981, The Clarkforkian Land Mammal Age and mammalian faunal composition across the Paleocene–Eocene boundary: University of Michigan Papers on Paleontology, v. 26, 197 p.
Rose, K.D., and Bown, T.M., 1982, New plesiadapiform primates from the Eocene of Wyoming and Montana: Journal of Vertebrate Paleontology, v. 2, p. 63–69.
Rose, K.D., and Gingerich, P.D., 1976, Partial skull of the plesiadapiform primate *Ignacius* from the early Eocene of Wyoming: Contributions from the Museum of Paleontology, University of Michigan, v. 24, p. 181–189.
Rose, K.D., Beard, K.C., and Houde, P., 1993, Exceptional new dentitions of the diminutive plesiadapiforms *Tinimomys* and *Niptomomys* (Mammalia), with comments on the upper incisors of Plesiadapiformes: Annals of Carnegie Museum, v. 62, p. 351–361.

https://doi.org/10.1017/jpa.2022.103 Published online by Cambridge University Press

Russell, D.E., Louis, P., and Savage, D.E., 1967, Primates of the French early Eocene: University of California Publications in Geological Sciences, v. 73, 46 p.
Russell, L.S., 1926, A new species of the genus *Catopsalis* Cope from the Paskapoo Formation of Alberta: American Journal of Science, v. 12, p. 230–234.
Russell, L.S., 1929, Paleocene vertebrates from Alberta: American Journal of Science, v. 17, p. 162–178.
Russell, L.S., 1967, Palaeontology of the Swan Hills area, northcentral Alberta: Royal Ontario Museum Life Sciences Contributions, v. 71, 31 p.
Rutherford, R.L., 1927, Geology along the Bow River between Cochrane and Kananaskis, Alberta: Scientific and Industrial Research Council of Alberta Report No. 17, 29 p.
Schiebout, J.A., 1974, Vertebrate paleontology and paleoecology of Paleocene Black Peaks Formation, Big Bend National Park, Texas: Texas Memorial Museum Bulletin 24, 88 p.
Scott, C.S., 2003, Late Torrejonian (middle Paleocene) mammals from south central Alberta, Canada: Journal of Paleontology, v. 77, p. 745–768.
Scott, C.S., 2008, Late Paleocene mammals from near Red Deer, Alberta, and a phylogenetic analysis of the earliest Lipotyphla (Mammalia, Insectivora) [Ph.D. dissertation]: Edmonton, University of Alberta, 1340 p.
Scott, C.S., 2010, *Eudaemonema webbi* sp. nov. (Mammalia, Mixodectidae) from the late Paleocene of western Canada: the youngest known mixodectid: Canadian Journal of Earth Sciences, v. 47, p. 1451–1462.
Scott, C.S., 2019, Horolodectidae: a new family of unusual eutherians (Mammalia: Theria) from the Palaeocene of Alberta, Canada: Zoological Journal of the Linnean Society, v. 185, p. 431–458.
Scott, C.S., and Fox, R.C., 2005, Windows on the evolution of *Picrodus* (Plesiadapiformes: Primates): morphology and relationships of a species complex from the Paleocene of Alberta: Journal of Paleontology, v. 79, 635–657.
Scott, C.S., Fox, R.C., and Youzwyshyn, G.P., 2002, New earliest Tiffanian (late Paleocene) mammals from Cochrane 2, southwestern Alberta, Canada: Acta Palaeontologica Polonica, v. 47, p. 691–704.
Scott, C.S., Spivak, D.N., and Sweet, A.R., 2013, First mammals from the Paleocene Porcupine Hills Formation of southwestern Alberta, Canada: Canadian Journal of Earth Sciences, v. 50, p. 355–378.
Secord, R., 2008, The Tiffanian Land-Mammal Age (middle and late Paleocene) in the northern Bighorn Basin, Wyoming: University of Michigan Papers on Paleontology, v. 35, 192 p.
Silcox, M.T., 2001, A phylogenetic analysis of the Plesiadapiformes and their relationship to Euprimates and other Archonta [Ph.D. dissertation]: Baltimore, The Johns Hopkins University, 723 p.
Silcox, M.T., 2003, New discoveries on the middle ear anatomy of *Ignacius graybullianus* (Paromomyidae, Primates) from ultra high resolution X-ray computed tomography: Journal of Human Evolution, v. 44, p. 73–86.
Silcox, M.T., 2008, The biogeographic origins of primates and euprimates: east, west, north, or south of Eden?, *in* Sargis, E.J., and Dagosto, M., eds., Mammalian Evolutionary Morphology: A Tribute to Frederick S. Szalay: New York, Springer-Verlag, p. 199–231.
Silcox, M.T., and Gunnell, G.F., 2008, Plesiadapiformes, *in* Janis, C.M., Gunnell, G.F., and Uhen, M.D., eds., Evolution of Tertiary Mammals of North America Vol. 2: Marine Mammals and Smaller Terrestrial Mammals: Cambridge, Cambridge University Press, p. 207–238.
Silcox, M.T., and Williamson, T.E., 2012, New discoveries of early Paleocene (Torrejonian) primates from the Nacimiento Formation, San Juan Basin, New Mexico: Journal of Human Evolution, v. 63, p. 805–833.
Silcox, M.T., Rose, K.D., and Bown, T.M., 2008, Early Eocene Paromomyidae (Mammalia, Primates) from the southern Bighorn Basin, Wyoming: systematics and evolution: Journal of Paleontology, v. 82, p. 1074–1113.
Silcox, M.T., Bloch, J.I., Boyer, D.M., Godinot, M., Ryan, T.M., Spoor, F., and Walker, A., 2009, Semicircular canal system in early primates: Journal of Human Evolution, v. 56, p. 315–327.
Silcox, M.T., Bloch, J.I., Boyer, D.M., and Houde, P., 2010, Cranial anatomy of Paleocene and Eocene *Labidolemur kayi* (Mammalia: Apatotheria) and the relationships of the Apatemyidae to other mammals: Zoological Journal of the Linnean Society, v. 160, p. 773–825.
Silcox, M.T., Bloch, J.I., Boyer, D.M., Chester, S.G., and López-Torres, S., 2017, The evolutionary radiation of plesiadapiforms: Evolutionary Anthropology, v. 26, p. 74–94.
Silcox, M.T., Gunnell, G.F., and Bloch, J.I., 2020, Cranial anatomy of *Microsyops annectens* (Microsyopidae, Euarchonta, Mammalia) from the middle Eocene of northwestern Wyoming: Journal of Paleontology, v. 94, p. 979–1006.
Simpson, G.G., 1940, Studies on the earliest primates: Bulletin of the American Museum of Natural History, v. 77, p. 185–212.
Simpson, G.G., 1955, The Phenacolemuridae, new family of early primates: Bulletin of the American Museum of Natural History, v. 105, p. 415–441.
Swofford, D.L., 2002, PAUP: Phylogenetic analysis using parsimony (and other methods), Version 4.0*a165: Sinauer Associates, http://paup.phylosolutions.com/
Szalay, F.S., 1969, Mixodectidae, Microsyopidae, and the insectivore–primate transition: Bulletin of the American Museum of Natural History, v. 140, p. 193–330.
Szalay, F.S., 1973, New Paleocene primates and a diagnosis of the new suborder Paromomyiformes: Folia Primatologica, v. 19, p. 73–87.
Szalay, F.S., and Delson, E., 1979, Evolutionary History of the Primates: New York, Academic Press, 580 p.
Szalay, F.S., and Drawhorn, G., 1980, Evolution and diversification of the Archonta in an arboreal milieu, *in* Luckett, W.P., ed., Comparative Biology and Evolutionary Relationships of Tree Shrews: New York, Plenum Press, p. 133–169.
Szalay, F.S., Rosenberger, A.L., and Dagosto, M., 1987, Diagnosis and differentiation of the order Primates: Yearbook of Physical Anthropology, v. 30, p. 75–105.
Tong, Y., and Wang, J., 1998, A preliminary report on the early Eocene mammals of the Wutu Fauna, Shandong Province, China, *in* Beard, K.C., and Dawson, M.R., eds., Dawn of the Age of Mammals in Asia: Bulletin of Carnegie Museum of Natural History, v. 34, p. 186–193.
Tong, Y., and Wang, J., 2006, Fossil mammals from early Eocene Wutu Formation of Shandong Province: Palaeontologia Sinica, new ser. C, v. 192, 201 p.
Van Valen, L., 1966, Deltatheridia, a new order of mammals: Bulletin of the American Museum of Natural History, v. 132, 126 p.
Van Valen, L., and Sloan, R.E., 1965, The earliest primates: Science, v. 150, p. 743–745.
West, R.M., and Dawson, M. R., 1977, Mammals from the Palaeogene of the Eureka Sound Formation: Ellesmere Island, Arctic Canada: Géobios, Mémoire Spécial, v. 1, p. 107–124.
Woodburne, M.O., 2004, Principles and procedures, *in* Woodburne, M.O., ed., Late Cretaceous and Cenozoic Mammals of North America: Biostratigraphy and Geochronology: New York, Columbia University Press, p. 1–20.
Youzwyshyn, G.P., 1988, Paleocene mammals from near Cochrane, Alberta [M. Sc. thesis]: Edmonton, University of Alberta, 484 p.

Accepted: 7 October 2022